doi.org/10.26434/chemrxiv.10073072.v1

Sterol Uptake by an Alkali-Beta-Cyclodextrin Metal-Organic Framework

Barry Blight, Towseef I Ahmad, Helena J. Shepherd, Christopher S. Jennings, Livia I Ferland, Simon J Teat, Jeremy S. Rossman

Submitted date: 29/10/2019 • Posted date: 31/10/2019

Sterol uptake by a new alkali-beta-cyclodextrin metal-organic framework that is comprised of stacked nanotubes made of beta-cyclodextrin.

Sterol Uptake by an Alkali-β-Cyclodextrin Metal-Organic Framework

Barry A. Blight,[a,b] Towseef I. Ahmad,[b] Helena J. Shepherd,[b] Christopher S. Jennings,[a] Livia I. Ferland,[a] Simon J. Teat[c] and Jeremy S. Rossman*[d]*

[a]Department of Chemistry, University of New Brunswick, Fredericton, N.B., E3B 5A3, Canada

[b]School of Physical Science, University of Kent, Canterbury, CT2 7NH, United Kingdom

[c]Advanced Light Source, Lawrence Berkeley National Lab, Berkeley, CA 94270, USA

[d]School of Bioscience, University of Kent, Canterbury, CT2 7NH, United Kingdom

KEYWORDS: coordination networks, metal-organic frameworks, cyclodextrin, cholesterol, organic molecule absorption

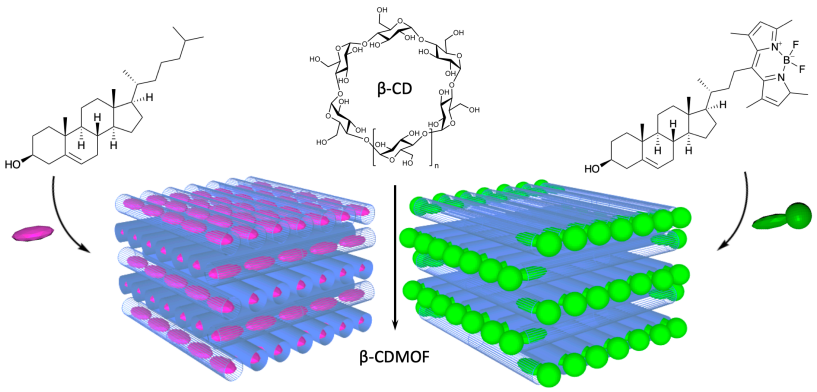

Abstract: β-Cyclodextrin is well known in cellular biology for its ability to moderate cholesterol levels in lipid bilayer membranes. Its use in extended network solids remains elusive due to the low symmetry of this macrocyclic system. Self-assembly of two different β-cyclodextrin MOFs with extended nanotube structures is achieved by crystallization with excess potassium hydroxide, one in the presence of cholesterol. We then further demonstrate the proclivity of one of these MOFs to absorb cholesterol and two other sterols from solution using NMR and confocal microscopy techniques. This work demonstrates that these network solids show great potential in both substrate delivery and/or extraction.

Cyclodextrins (CDs) are a unique class of material with uses spanning the biological, chemical and materials sciences. The three most common forms of CD are comprised of six (α-), seven (β-), and eight (γ-) 1,4-linked pyranose units giving rise to cylindrical-shaped structures with hydrophilic exterior and a hydrophobic core. Their unique three-dimensional shape offer materials scientists several chemical handles for functionalization, and predictable behaviour with the primary and secondary faces of the toroid pointed with equatorially disposed glycosidic 1,3- and 1,2-diols, respectively (Figure 1).[1–4] Ideally positioned for meta-ligand chelation, the development of coordination networks that incorporate the toroidal motif in a manner that gives rise to extended ordered porosity has received notable interest in recent years.[5] While there is still substantial untapped promise in the use of these sugar-centric network solids (also referred to as metal-organic frameworks; in this case CD-MOFs), to date they have demonstrated limited success beyond carbon dioxide uptake,[6,7] gold ion extraction,[8,9] separating small chiral / aromatic compounds,[10,11] and mediated drug release.[12,13] This is in contrast to myriad of other applications that now employ multi-topic carboxylate-linked MOFs including but not limited to gas-sorption/separation,[14,15]

water sorption,[16] catalysis,[17] sensing,[18,19] and drug delivery.[20,21] Few of these systems, however, are derived entirely from renewable or naturally available components,[22–26] making the pursuit of CD-based MOFs with demonstrable utility particularly important. While the components of CD-based MOFs would be considered naturally occurring and/or derived from renewable resources, very few have demonstrated usefulness within -or interacting with components of- the biological arena.[12,27] We found this particularly intriguing considering the important role that β-CD plays in biochemical research. It has been well documented that β-CD and by extension, methyl-β-CD (MBCD) have become quintessential tools in the mediation of intralamellar cholesterol levels from outside the membrane environment in order to influence cholesterol-dependent cellular processes.[28] For example, MBCD has been used to treat tissue culture cells to control cholesterol-dependent budding of influenza viruses,[29] and was separately demonstrated to modulate cholesterol interaction with the in-membrane oxytocin receptor protein.[30] In parallel and of particular importance in medical research, is the study of β-CDs as potential lipoprotein mimics by moderating in vivo cholesterol metabolism for combating atherosclerosis.[31–33] Through the formation of a [n]pseudorotaxane-style host-guest (HG) inclusion complex, hydrophilic β-CD solubilizes the highly hydrophobic sterol (and others) in aqueous environments with a remarkable association constant of $K_a = 1.7 \times 10^4\ M^{-1}$, as determined by the spectral displacement method.[34] In fact, this is such an effective solubilizing system that a β-CD-cholesterol HG-complex is commercially available from a number of suppliers as 'Cholesterol Water Soluble'.

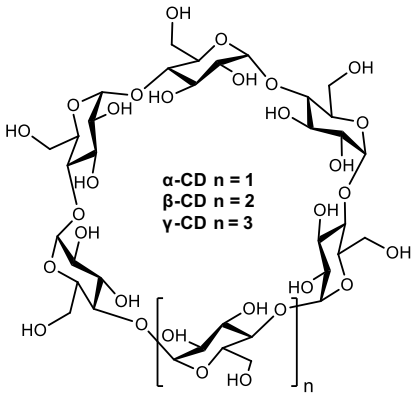

Figure 1. General structure of the three most common commercially available cyclodextrins.

In this account, we report the self-assembly of two new β-cyclodextrin-centered MOFs with apertures that align to form extended nanotubular arrays; one of which includes full characterization due to its broader HG applications (β-CDMOF-**1**) comprised of β-CD and K^+. Separately, crystalline β-CDMOF-**2**•Chol was grown in the presence of cholesterol and structure confirmed by single crystal XRD, a first for this particular HG complex as an extended network and only the second time as a discrete HG complex.[35] This is surprising considering the ubiquitous use of the β-CD-cholesterol complex in biology and across multiple divisions of chemistry.[36,37] Second, we demonstrate that (β-CDMOF-**1** is capable of extracting cholesterol (along with other sterols) from solution into the extended network pores of the sugar-based nanotube structures, and further examine the crystal sponge behaviour by BODIPY-labelled cholesterol and separately resorufin uptake by fluorescence microscopy.

Self-assembly of β-CDMOF-**1** and -**2**•Chol was achieved by slow solvent diffusion (either vapour or layering as noted) of methanol into combined aqueous solutions of β-CD (1.0 eq.) and potassium hydroxide (KOH; 20 eq.) in the presence or absence of desired the guest species. Crystal growth of described topologies was highly reproducible, and achieved within a 5-day timeframe.

Inspired by the works of Stoddart and coworkers,[26] we began the studies by attempting to assemble the networks with potassium hydroxide. The challenge with crystallizing any extended arrays of β-CD would be the decreased symmetry due to the C7-rotational symmetry of β-CD.

β-CDMOF-**1** crystallized in Triclinic *P1* space group as colorless plates that grow from a central point, resulting in starburst-shaped crystal clusters in an 83% yield. The asymmetric unit is comprised of four crystallographically distinct β-CD toroids, which form cylindrical nanotubes through head-to-head / tail-to-tail complimentary H-bonding interactions between primary and secondary alcohol moieties on each rim of the molecules. The nanotubes are linked together into 2-dimensional sheets of parallel nanotubes, and adjacent sheets are aligned at 95° to one another through coordination of nine crystallographically unique potassium ions. The porosity of this structure thus extends infinitely along the a- and b-axes in discrete channels through the interior of the β-CD channels, as shown in Figure 2.

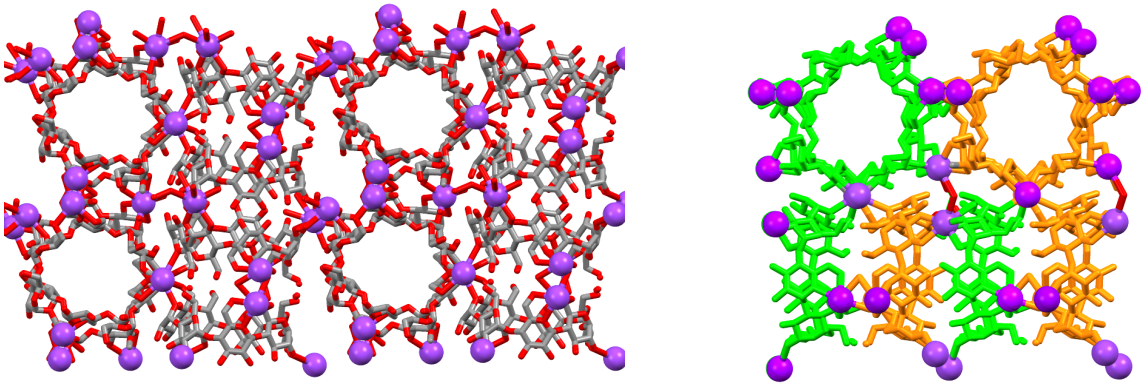

Figure 2. Two separate visualisations of β-CDMOF-**1**. Left: expanded view of network lattice; Right: condensed view of network lattice with colored β-CD rings to demonstrate topological alignment. In both images, hydrogen atoms and water molecules are removed for clarity. Potassium, purple; carbon, grey; oxygen, red.

Volatility of the methanol supernatant resulted in rapid solvent loss of the crystals and disintegration of the crystal lattice. Removal of the supernatant and soaking in ethanol for 24 hours followed by two 24-hour dichloromethane soaks afforded starburst crystals stable enough to be easily handled for TGA, elemental analysis, and X-ray powder diffraction (see supporting information). In fact, the DCM soaking protocol was demonstrated by TGA to slightly increase the thermal stability of the coordination assembly (See SI, Fig. S3), though any solvent loss adversely affected the extended crystallinity of the material as seen in the X-ray powder diffraction. Porosimetry experiments were unsuccessful, as the material was not stable enough to withstand the activating conditions required. Nonetheless, surface area was estimated using low level Connolly Surface calculation to be 1250 m^2g^{-1}, using the single crystal diffraction data. When the material remained solvated, however, the crystals remained intact and could be easily handled and transferred between vessels.

β-CDMOF-**2**•Chol crystallized as colorless cuboid crystals in a Monoclinic $P2_1$ space group with β-CD units aligned to form parallel one-dimensional nanotubes, with primary and secondary faces of the CD toroids again assembled in a head-to-head / tail-to-tail arrangement, stabilized by several complimentary H-bonds at each interfacial junction. Three potassium ions (one of which is partially occupied) participate in inter-nanotube coordination, forming a network of parallel nanotubes along the unit cell's *a*-axis. The pores of these tubes contain guest cholesterol molecules (1/3 occupancy for each pair of CD host molecules; thus 1:6 cholesterol/β-CD ratio), which have been crystallographically characterized in-situ, as shown in Figure 3. The observation of cholesterol within the pores suggests that these networks may be capable of cholesterol uptake in the form of a crystal sponge.[38] Considering that the conditions for assembly of β-CDMOF-**2**•Chol mirrored that of β-CDMOF-**1**, we posit that the presence of cholesterol contributed in the

templating of the parallel one-dimensional porous network, an attribute we are currently exploring. Investigation of the structure reveals no significant intermolecular interactions between any cholesterol functionality and the interior walls of the CD channels. Specifically to this structure, we see no hydrogen bond contacts to the free secondary alcohol of cholesterol by any β-CD oxygen. As this is a coordination network and not a solvated intermolecular HG system, the two environments are not comparable but this observation supports conclusions that a driving force for the solvated HG assembly is predominantly by solvophobic Van der Waals' attraction.

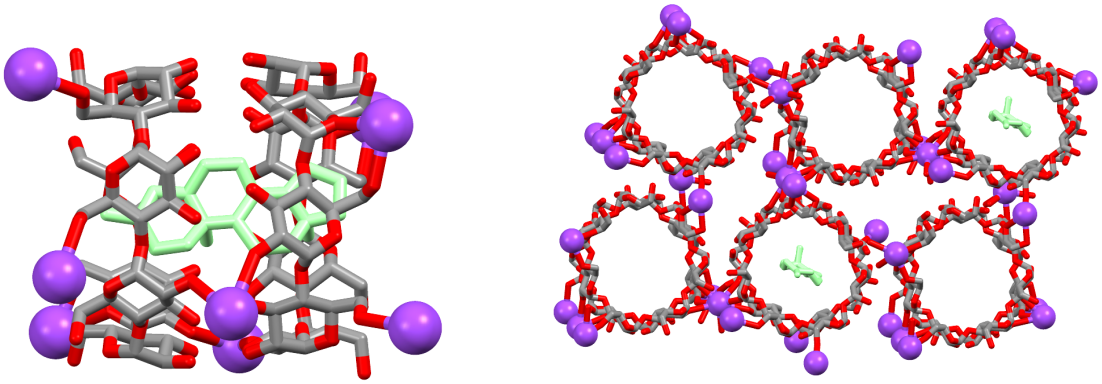

Figure 3. Visualization of β-CDMOF-**2**•Chol containing one-third cholesterol occupancy. Left: asymmetric unit exhibiting guest binding of cholesterol within the β-CDMOF pores, looking down c-axis; Right: expanded view of the lattice network looking down the b-axis. Hydrogen atoms, water molecules, and the disordered cholesterol alkyl-chain are removed for clarity. Potassium, purple; carbon, grey; oxygen, red; cholesterol, green.

To examine the uptake of molecular cholesterol from solution, we first chose to established the stability of the crystal morphology during the cholesterol soaking process compared to 'free' crystalline β-CD. Soaking of β-CD crystals in an ethanolic solution of cholesterol resulted in the visible crystallization of cholesterol on the surface of the non-porous close-packed β-CD solid

(See SI, Fig. S5). Single crystal diffraction analysis of these hybrid crystals revealed a single crystal pattern indistinguishable from that of β-CD, superimposed with a powder diffraction pattern of cholesterol originating in the crystallites that had grown on the surface. This indicates that cholesterol does not penetrate into β-CD crystals, rather interacting with the surface only. However, soaking of β-CDMOF-**1** under the same conditions resulted in unchanged crystal morphology, presumably because the network solid is being loaded with cholesterol instead of nucleating on the surface.

^{1}H NMR analysis of the digested solids followed to assess this behaviour. Again, crystals of β-CDMOF-**1** were soaked in an ethanolic solution of cholesterol for 24 hours, the supernatant removed, and crystals rinsed twice to dissolve away any surface adsorbed cholesterol with remaining solvent being removed in-vacuo. The β-CDMOF-**1** solids were then digested in the chosen NMR solvents to assess host-guest ratios in identifying degree of cholesterol uptake. This analysis revealed an approximate ratio of 2:1 β-CD to cholesterol (Figure 4a) by integration of the respective ^{1}H NMR signals. We surmise that this ratio is too large to be merely surface adsorption of cholesterol to the crystal surface (particularly after a rinsing protocol), nor do we feel any accessible crystal fracture planes would accommodate cholesterol due to the highly ionic nature of the adjoining space between the nanotubular arrays. This study was also extended to include deoxycholic acid, β-estradiol, and a size-comparable dye molecule named resorufin (Figure 4b). The two related sterols showed similar uptake capacities (3:1 β-CD to deoxycholic acid and 14:1 β-CD to β-estradiol; see SI, Section 6) establishing that β-CDMOF-**1** does indeed demonstrate crystal sponge behaviour. The root cause of this host-guest interaction is largely driven by solvophobic effects due to high polarity of the ethanol solvent and low polarity of the β-CD nanotubes. This is comparable to the complexation of free β-CD or MBCD with cholesterol in

water (a well-documented system).[34] In contrast, we see no uptake of resorufin by NMR analysis, for which we attribute this to its smaller size (fewer Van der Waal's interactions) and much higher localized polarity.

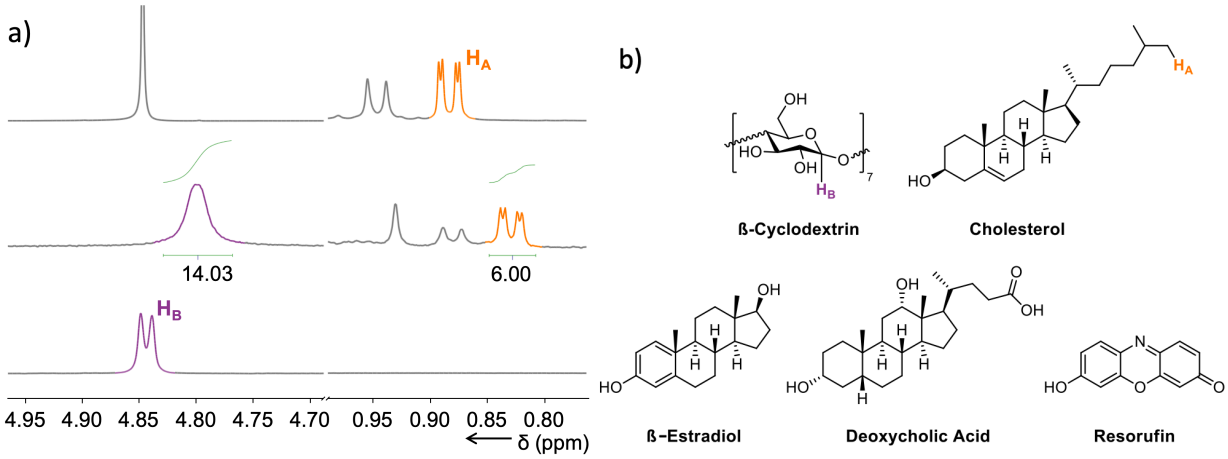

Figure 4. (a) Selected peaks from the ^{1}H NMR spectra of cholesterol (methanol-d_4, 400 MHz, top) cholesterol-soaked β-CDMOF-**1** (digested in methanol-d_4/ DMSO-d_6, 400 MHz, middle) and β-CD (methanol-d_4/ DMSO-d_6, 400 MHz, bottom). Full spectra shown in Fig. S6 (see SI). (b) Molecular structures of β-CD and sterol guest molecules in this study. Proton environments that give rise to the peaks in Fig. 4a are highlighted for β-CD (purple) and cholesterol (orange).

Since ^{1}H NMR is not direct evidence of cholesterol uptake, and SCXRD on cholesterol-soaked crystals afforded pore contents of intractable disorder, further evidence of this phenomenon was collected using fluorescence confocal microscopy, by employing guest molecules containing strongly emitting fluorophores (Figure 5). To accomplish this, we chose to employ commercial Bodipy-cholesterol (BO-C), which is as the name suggests, a Bodipy-conjugated cholesterol commonly used in cell imaging,[39] and separately, the aforementioned resorufin dye. The distinction between the two emitters is wavelength of emission maximum (507 nm and 586 nm, respectively) and molecular size (Bodipy is a large pendant group, while resorufin is small and

initially thought to permeate through the pores). Samples of β-CDMOF-**1** were loaded with each respective substrate in accordance with the above NMR analysis procedures, followed by crystal selection for microscopy. The samples were thoroughly rinsed to limit background fluorescence of free substrate and analyzed under a blanket of ethanol to prevent desolvation.

Quantitative analysis of β-CDMOF-**1**•BO-C reveals that emission properties of BO-C are more prominent on the crystal edges (*a*-axis) due to cumulative intensity of the higher fluorescence signal along the crystal edges (Figure 5a). Here, BO-C can bind on the surface by inclusion of the cholesterol portion, but not totally enter caused by the restrictive size of the Bodipy moiety. Intensity mapping illustrates this phenomenon with some emission intensity along the *b*-axis (crystal face), but with lower intensity, indication of a single layer (or lower cumulative concentration) of fluorophore. This image visually illustrates the surface inclusion of BO-C. Analysis of β-CDMOF-**1**•resorufin revealed quite different behaviour (Figure 5b). As noted in the NMR analysis, it was initially posited that the resorufin dye was of sufficient size to be included in the extended β-CD pores, however, this was not observed upon digestion of the MOF material. Confocal analysis revealed that that resorufin appears to permeate into the crystal fracture planes, which would presume to be areas of high polarity (opposite of what would be found inside the β-CD pores. Fluorescence intensity mapping revealed quite regular peak intensities across the crystal surface, indicative of dye being situated within the orthogonal crystal grain dislocations where the sugar oxides and potassium ions reside, rather than being restricted to the surface. This result nicely contrasts that of the inclusion of BO-C and further demonstrates the proclivity of cholesterol uptake in this unique system.

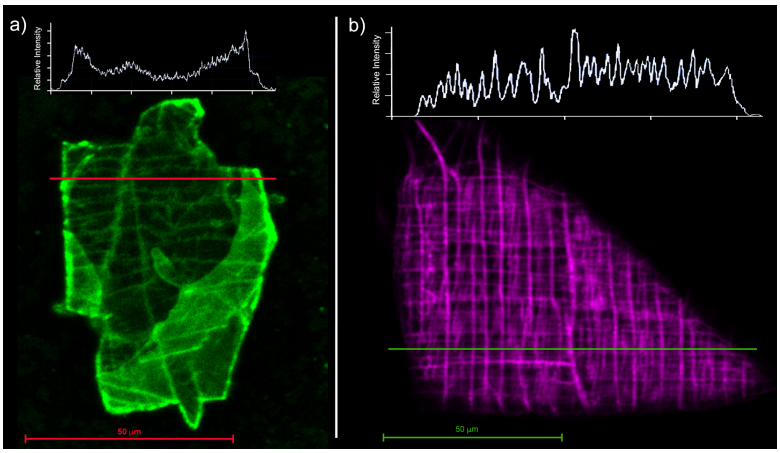

Figure 5. Confocal images of β-CDMOF-**1** crystals loaded with a) Bodipy-cholesterol (λ_{exc} = 488 nm, emission filters: BP 420-480 nm and BP 495-620 nm and b) resorufin dyes (λ_{exc} = 561 nm, emission filters: BP 570-620 nm and LP 645 nm). Inset: fluorescence intensity profiles illustrating dye dispersion.

In conclusion, we have presented two new cyclodextrin-based MOFs employing β-CD as the structural building unit, one of which containing cholesterol within its pores. We also demonstrate that β-CDMOF-**1** is capable of sterol uptake within its non-polar pores, and are able to contrast this be behaviour with similarly-sized dye molecule that exhibited no uptake tendency. This work lays the foundation for our group to develop new MOF technologies related to extraction therapeutics, in this case, towards the combating of Atherosclerosis, and the potential for delivery of steroidal drugs.

ASSOCIATED CONTENT

Supporting Information. The supporting information are available free of charge. In addition, X-ray structural data has been uploaded to the Cambridge Crystallographic Database.

Experimental details with additional figures and tables (PDF)

X-ray data for β-CDMOF-**1** (CCDC-1959832) and β-CDMOF-**2**•Chol (CCDC-1959833) (CIF)

AUTHOR INFORMATION

Corresponding Author

*Email: b.blight@unb.ca

ORCID

Barry A. Blight 0000-0003-1166-6206
Helena J. Shepherd 0000-0003-0832-4475
Simon J. Teat 0000-0001-9515-2602
Jeremy S. Rossman 0000-0001-6124-4103

Notes

The authors declare no competing financial interests.

ACKNOWLEDGMENT

The authors are grateful for support from the University of Kent and the University of New Brunswick. TIA was funded by a University of Kent, School of Physical Science tuition scholarship and CSJ was funded by the New Brunswick Foundation for Innovation (NBIF) Research Assistant Initiative.

REFERENCES

(1) Rey-Rico, A.; Cucchiarini, M. Supramolecular Cyclodextrin-Based Hydrogels for Controlled Gene Delivery. *Polymers (Basel)*. **2019**, *11* (3), 514–519.

(2) Osman, S. K.; Brandl, F. P.; Zayed, G. M.; Teßmar, J. K.; Göpferich, A. M. Cyclodextrin Based Hydrogels: Inclusion Complex Formation and Micellization of Adamantane and Cholesterol Grafted Polymers. *Polymer (Guildf)*. **2011**, *52* (21), 4806–4812.

(3) Schmidt, B.; Barner-Kowollik, C. Dynamic Macromolecular Material Design - The Versatility of Cyclodextrin Based Host/Guest Chemistry. *Angew. Chemie Int. Ed.* **2017**, 1–21.

(4) Zhang, Y.-M.; Liu, Y.-H.; Liu, Y. Cyclodextrin-Based Multistimuli-Responsive Supramolecular Assemblies and Their Biological Functions. *Adv. Mater.* **2019**, *453*, 1806119–1806158.

(5) Rajkumar, T.; Kukkar, D.; Kim, K.-H.; Sohn, J. R.; Deep, A. Cyclodextrin-Metal–Organic Framework (CD-MOF): From Synthesis to Applications. *J. Ind. Eng. Chem.* **2019**, *72*, 50–66.

(6) Forgan, R. S.; Smaldone, R. A.; Gassensmith, J. J.; Furukawa, H.; Cordes, D. B.; Li, Q.; Wilmer, C. E.; Botros, Y. Y.; Snurr, R. Q.; Slawin, A. M. Z.; et al. Nanoporous Carbohydrate Metal–Organic Frameworks. *J. Am. Chem. Soc.* **2012**, *134* (1), 406–417.

(7) Gassensmith, J. J.; Furukawa, H.; Smaldone, R. A.; Forgan, R. S.; Botros, Y. Y.; Yaghi, O. M.; Stoddart, J. F. Strong and Reversible Binding of Carbon Dioxide in a Green Metal–Organic Framework. *J. Am. Chem. Soc.* **2011**, *133* (39), 15312–15315.

(8) Liu, Z.; Samanta, A.; Lei, J.; Sun, J.; Wang, Y.; Stoddart, J. F. Cation-Dependent Gold Recovery with α-Cyclodextrin Facilitated by Second-Sphere Coordination. *J. Am. Chem. Soc.* **2016**, *138* (36), 11643–11653.

(9) Liu, Z.; Frasconi, M.; Lei, J.; Brown, Z. J.; Zhu, Z.; Cao, D.; Iehl, J.; Liu, G.; Fahrenbach, A. C.; Botros, Y. Y.; et al. Selective Isolation of Gold Facilitated by Second-Sphere Coordination with a-Cyclodextrin. *Nat. Commun.* **1AD**, *4*, 1855–1859.

(10) Hartlieb, K. J.; Holcroft, J. M.; Moghadam, P. Z.; Vermeulen, N. A.; Algaradah, M. M.; Nassar, M. S.; Botros, Y. Y.; Snurr, R. Q.; Stoddart, J. F. CD-MOF: A Versatile Separation Medium. *J. Am. Chem. Soc.* **2016**, *138* (7), 2292–2301.

(11) Yang, C.-X.; Zheng, Y.-Z.; Yan, X.-P. γ-Cyclodextrin Metal–Organic Framework for Efficient Separation of Chiral Aromatic Alcohols. *RSC Adv.* **2017**, *7* (58), 36297–36301.

(12) Hartlieb, K. J.; Ferris, D. P.; Holcroft, J. M.; Kandela, I.; Stern, C. L.; Nassar, M. S.; Botros, Y. Y.; Stoddart, J. F. Encapsulation of Ibuprofen in CD-MOF and Related Bioavailability Studies. *Mol. Pharm.* **2017**, *14* (5), 1831–1839.

(13) Sha, J.; Yang, X.; Sun, L.; Zhang, X.; Li, S.; Li, J.; Sheng, N. Unprecedented α-Cyclodextrin Metal-Organic Frameworks with Chirality: Structure and Drug Adsorptions. *Polyhedron* **2017**, *127*, 396–402.

(14) Ma, L.; Svec, F.; Lv, Y.; Tan, T. Engineering of the Filler/Polymer Interface in Metal–Organic Framework-Based Mixed-Matrix Membranes to Enhance Gas Separation. *Chem. - An Asian J.* **2019**, *311*, 614–639.

(15) Zhang, Z.; Cano, Z. P.; Luo, D.; Dou, H.; Yu, A.; Chen, Z. Rational Design of Tailored Porous Carbon-Based Materials for CO 2 Capture. *J. Mater. Chem. A* **2019**, *7* (37), 20985–21003.

(16) Hanikel, N.; Prévot, M. S.; Fathieh, F.; Kapustin, E. A.; Lyu, H.; Wang, H.; Diercks, N. J.; Glover, T. G.; Yaghi, O. M. Rapid Cycling and Exceptional Yield in a Metal-Organic Framework Water Harvester. *ACS Cent. Sci.* **2019**.

(17) Wasson, M. C.; Buru, C. T.; Chen, Z.; Islamoglu, T.; Farha, O. K. Metal–Organic Frameworks: A Tunable Platform to Access Single-Site Heterogeneous Catalysts. *Appl. Catal. A Gen.* **2019**, *586* (May), 117214. https://doi.org/10.1016/j.apcata.2019.117214.

(18) Koo, W.-T.; Jang, J.-S.; Kim, I.-D. Metal-Organic Frameworks for Chemiresistive Sensors. *Chem* **2019**, 1–26.

(19) Yan, B. Photofunctional MOF-Based Hybrid Materials for the Chemical Sensing of Biomarkers. *J. Mater. Chem. C* **2019**, *7* (27), 8155–8175.

(20) Zhang, Z.; Sang, W.; Xie, L.; Dai, Y. Metal-Organic Frameworks for Multimodal Bioimaging and Synergistic Cancer Chemotherapy. *Coord. Chem. Rev.* **2019**, *399*, 213022.

(21) zaro, I. A. nades L. Ã.; Forgan, R. S. Application of Zirconium MOFs in Drug Delivery and Biomedicine. *Coord. Chem. Rev.* **2019**, *380*, 230–259.

(22) Rabone, J.; Yue, Y. F.; Chong, S. Y.; Stylianou, K. C.; Bacsa, J.; Bradshaw, D.; Darling, G. R.; Berry, N. G.; Khimyak, Y. Z.; Ganin, A. Y.; et al. An Adaptable Peptide-Based

Porous Material. *Science (80)* **2010**, *329* (5995), 1053–1057.

(23) Martí-Gastaldo, C.; Warren, J. E.; Stylianou, K. C.; Flack, N. L. O.; Rosseinsky, M. J. Enhanced Stability in Rigid Peptide-Based Porous Materials. *Angew. Chemie Int. Ed.* **2012**, *51* (44), 11044–11048.

(24) Katsoulidis, A. P.; Park, K. S.; Antypov, D.; Martí-Gastaldo, C.; Miller, G. J.; Warren, J. E.; Robertson, C. M.; Blanc, F.; Darling, G. R.; Berry, N. G.; et al. Guest-Adaptable and Water-Stable Peptide-Based Porous Materials by Imidazolate Side Chain Control. *Angew. Chemie Int. Ed.* **2013**, *53* (1), 193–198.

(25) Huskic, I.; Pekov, I. V; Krivovichev, S. V; Friscic, T. Minerals with Metal-Organic Framework Structures. *Sci. Adv.* **2016**, *2* (8), e1600621–e1600621.

(26) Smaldone, R. A.; Forgan, R. S.; Furukawa, H.; Gassensmith, J. J.; Slawin, A. M. Z.; Yaghi, O. M.; Stoddart, J. F. Metal-Organic Frameworks from Edible Natural Products. *Angew. Chemie Int. Ed.* **2010**, *49* (46), 8630–8634.

(27) Sha, J.-Q.; Zhong, X.-H.; Wu, L.-H.; Liu, G.-D.; Sheng, N. Nontoxic and Renewable Metal–Organic Framework Based on α-Cyclodextrin with Efficient Drug Delivery. *RSC Adv.* **2016**, *6* (86), 82977–82983.

(28) Ohtani, Y.; Pitha, J.; Irie, T.; Uekama, K.; Fukunaga, K. Differential Effects of α-, β- and γ-Cyclodextrins on Human Erythrocytes. *Eur. J. Biochem.* **1989**, *186*, 17–22.

(29) Rossman, J. S.; Jing, X.; Leser, G. P.; Lamb, R. A. Influenza Virus M2 Protein Mediates ESCRT-Independent Membrane Scission. *Cell* **2010**, *142* (6), 902–913.

(30) Klein, U.; Gimpl, G.; Fahrenholz, F. Alteration of the Myometrial Plasma Membrane Cholesterol Content with .Beta.-Cyclodextrin Modulates the Binding Affinity of the Oxytocin Receptor. *Biochemistry* **1995**, *34* (42), 13784–13793.

(31) Rothblat, G. H.; Christian, A. E.; Byun, H.-S.; Zhong, N.; Wanunu, M.; Marti, T.; Fürer, A.; Diedrich, F.; Bittman, R. Comparison of the Capacity of -Cyclodextrin Derivatives and Cyclophanes to Shuttle Cholesterol between Cells and Serum Lipoproteins. *J. Lipid Res.* **1999**, *40*, 1475–1482.

(32) Rothblat, G. H.; Christian, A. E.; Hayes, M. P.; Phillips, M. C. Use of Cyclodexrtrins for Manipulating Cholesterol Content. *J. Lipid Res.* **1997**, *38*, 2264–2272.

(33) Kilsdonk, E. P.; Yancey, P. G.; Stoudt, G. W.; Bangerter, F. W.; Johnson, W. J.; Phillips, M. C.; Rothblat, G. H. Cellular Cholesterol Efflux Mediated by Cyclodextrins. *J. Biol. Chem.* **1995**, *270* (29), 17250–17256.

(34) Selvidge, L. A.; Eftink, M. R. Spectral Displacement Techniques for Studying the Binding of Spectroscopically Transparent Ligands to Cyclodextrins. *Anal. Biochem.* **1986**, *154*, 400–408.

(35) Christoforides, E.; Papaioannou, A.; Bethanis, K. Crystal Structure of the Inclusion Complex of Cholesterol in β-Cyclodextrin and Molecular Dynamics Studies. *Beilstein J. Org. Chem.* **2018**, *14*, 838–848.

(36) Zhang, J.; Sun, H.; Ma, P. X. Host–Guest Interaction Mediated Polymeric Assemblies: Multifunctional Nanoparticles for Drug and Gene Delivery. *ACS Nano* **2010**, *4* (2), 1049–1059.

(37) Liu, J.; Alvarez, J.; Ong, W.; Esteban Román, A.; Kaifer, A. E. *Phase Transfer of Hydrophilic, Cyclodextrin-Modified Gold Nanoparticles to Chloroform Solutions*; American Chemical Society, 2001.

(38) Inokuma, Y.; Yoshioka, S.; Ariyoshi, J.; Arai, T.; Fujita, M. Preparation and Guest-Uptake Protocol for a Porous Complex Useful for "crystal-Free" Crystallography. *Nat. Protoc.* **2014**, *9* (2), 246–252.

(39) Hölttä-Vuori, M.; Uronen, R.-L.; Repakova, J.; Salonen, E.; Vattulainen, I.; Panula, P.; Li, Z.; Bittman, R.; Ikonen, E. BODIPY-Cholesterol: A New Tool to Visualize Sterol Trafficking in Living Cells and Organisms. *Traffic* **2008**, *9* (11), 1839–1849.

SUPPORTING INFORMATION

Sterol Uptake a β-Cyclodextrin Metal-Organic Framework

Barry A. Blight,*[a,b] Towseef I. Ahmad,[b] Helena J. Shepherd,[b] Christopher S. Jennings,[a] Livia I. Ferland,[a] Simon J. Teat[c] and Jeremy S. Rossman,*[d]

[a]Department of Chemistry, University of New Brunswick, Toole Hall
Fredericton, NB, E3B 5A3, Canada
Email: B.Blight@unb.ca
[b]School of Physical Sciences, University of Kent, Ingram Building,
Canterbury, CT2 7NH, UK.
[c]Advanced Light Source, Lawrence Berkeley National Lab,
Berkeley, CA 94270, USA
[d]School of Biosciences, University of Kent, Ingram Building,
Canterbury, CT2 7NH, UK.

Table of Contents:

S1. General Experimental Remarks

All chemicals and solvents were purchased from Alfa Aesar, Fisher Scientific, Avanti, Sigma-Aldrich and/or VWR and used without further purification.

Powder X-Ray Diffraction (PXRD): PXRD measurements were carried out at 298 K using a Rigaku benchtop X-ray diffractometer (λ (CuKα) = 1.5405 Å) on a zero-background holder. Data were collected over the range 3–45°. (University of Kent)

Single Crystal X-Ray Diffraction (SCXRD): a suitable crystal of ***β*-CDMOF** was selected and mounted on a Rigaku Oxford Diffraction Supernova diffractometer. Data were collected using Cu Kα radiation to a maximum resolution of 0.84 Å. Crystal was kept at 100(1) K during data collection using an Oxford Cryosystems 800-series Cryostream. The structure was solved with the ShelXT [S1] structure solution program using Direct Methods and refined with ShelXL [S2] via Least Squares minimisation. Olex2 [S3] was used as an interface to all ShelX programs.

ALC Beamline Single Crystal Diffraction:
X-ray diffraction data for ***β*-CDMOF-1** were collected on beamline 11.3.1 at the Advanced Light Source, Berkley, CA, U.S.A using Si (111) monochromated radiation at λ = 0.8856 Å on a Bruker AXS D8 three-circle diffractometer equipped with a Bruker AXS PHOTON 100 CMOS detector at 100 K. The sample temperature was controlled using an Oxford Cryosystems Cryostream Plus. The data were collected with CrysAlis Pro software[S4] and processed using Bruker AXS Apex2 software[S5] with SADABS-2014/15.[S6]

Elemental Analysis: CHN analysis was obtained using the London Metropolitan University Elemental Analysis Service in the School of Human Science: School of Human Sciences London Metropolitan University, 166-220 Holloway Road, Islington, N7 8DB, UK.

Thermal Gravimetric Analysis (TGA): Measurements were carried out using a NETZSCH STA 409 PC/PG apparatus. Measurements were collected from room temperature to 450 °C with a heating rate of 10 °C / min under an air atmosphere. (University of Kent)

Nuclear Magnetic Resonance Spectroscopy (NMR): NMR spectra were recorded on a JOEL NMR 400 MHz spectrometer and referenced to residual solvent peaks. (University of Kent)

Fluorescence Imaging: Confocal imaging was collected on a Zeiss Elyra P1. LSM880 Airyscan Fast Super resolution confocal system with the Airyscan detector to acquire the images. Fluorescent dyes used included Topfluor-Cholesterol (from Avanti) and Resorufin (from Sigma-Aldrich).

S2. β-Cyclodextrin network syntheses

***β*-CDMOF-1:** β-cyclodextrin (0.5675 g, 0.5 mmol) and potassium hydroxide (0. 5610g, 10 mmol) was added to a 10 ml volumetric flask and dissolved in de-ionised water (10 ml). Then 1 ml of this mixture was added to a 2 ml borosilicate sample vial. The 2 ml sample vial was placed in a 14 ml sample vial which contained 2.5 ml methanol. This system was sealed with a cap and set aside for crystal formation (4-5 days; 83% yield based on molar quantity in a single vial). Colourless crystals grew as long needles with multiple needles nucleating from a single point in 'starburst-like' crystal clusters. Crystals lost solvent quickly, as such solvent exchange allowed for a variety of characterisation methods. For single crystal X-ray diffraction and confocal analysis, crystals were washed once with absolute ethanol, solvent removed and then soaked in a fresh vial of absolute ethanol for 24 hours. For TGA and CHN analysis, the crystals were soak for a further 24 hours in a vial of DCM, followed by removal of the solvent and evacuated. Stability of crystals, post DCM soak, was markedly improved out of solvent. Elemental Analysis for $C_{168}H_{295}O_{152}K_9$ (4βCD·9KOH·4H_2O) calc: C: 39.43, H: 5.85, N: 0.0; found: C: 39.59, H: 5.69, N: 0.0.

Crystal data for *β*-CDMOF-1: $C_{42.5}H_{72}$ $K_{2.25}O_{41}$, M_r = 1326.97, crystal dimensions 0.07 × 0.04 × 0.04 mm, Triclinic, a = 15.2438(6) (2) Å, b = 15.2742(6) Å, c = 29.7686(13) Å, α = 101.314(2)° β = 94.845(2)°, γ = 95.071(2)°, V = 6733.1(5) Å^3, T = 100 K, space group $P1$, Z = 4, 62688 measured reflections, 50757 unique (R_{int} = 0.0473), which were used in all calculations. The final R_1 = 0.1136 for 50757 observed data $R[F^2 > 2\sigma(F^2)]$ and $wR(F^2)$ = 0.2964 (all data). Approximately 66% of the cell volume is not occupied by the framework and contains diffuse and disordered solvent molecules. This electron density was accounted for

using SQUEEZE within PLATON[S16] which calculated a solvent accessible volume of 20904 Å^3 containing 6114 electrons (the equivalent of ~153 molecules of methanol) per unit cell. Crystal structure data for **Zr-L2** are available from the CCDC, deposition number CCDC-1959832.

***β*-CDMOF-2:** β-cyclodextrin (0.262 g, 0.25 mmol) and potassium hydroxide (0.280 g, 5 mmol) was added to a 5 ml volumetric flask and dissolved in de-ionised water (5 ml). Then 1 ml of this mixture was added to a 5 mm NMR tube. 0.2 ml of deionised water, followed by 0.2 ml of methanol were was carefully layered on top of the *β*-CD/KOH solution. Separately, a 5 ml solution of cholesterol dissolved in methanol was prepared (0.125 mmol) and 1 ml of this solution was carefully layered on top. The sample was left for 3 weeks upon which 3 different sets of crystals appeared. Large colourless cubes crystallographically ascribed to *β*-CD on the bottom of the tube, very long colourless needles (some the length of the NMR tube) ascribed to cholesterol, and few small colourless cube-shaped single crystals that grew in the water/methanol interface. One of these single crystals was selected for SCXRD analysis.

Crystal data for *β*-CDMOF-2: $C_{96.64}H_{153.72}K_{2.25}O_{41}$, M_r = 2676.57, crystal dimensions 0.5 × 0.5 × 0.5 mm, Triclinic, a = 15.73558(13) (2) Å, b = 24.3380(2) Å, c = 19.02257(18) Å, α = 90° β = 107.6098(9)°, γ = 90°, V = 6943.73(11) Å^3, T = 100 K, space group $P2_1$, Z = 2, 122292 measured reflections, 24291 unique (R_{int} = 0.0392), which were used in all calculations. The final R_1 = 0.1051 for 24291 observed data $R[F^2 > 2\sigma(F^2)]$ and $wR(F^2)$ = 0.2845 (all data). Structure was successfully modelled with cholesterol carrying one third occupancy equating to one cholesterol molecule for every six cyclodextrin molecules. Crystal structure data for ***β*-CDMOF-2** are available from the CCDC, deposition number CCDC-1959833.

S3. Powder X-ray Diffraction

Powder X-ray diffraction (PXRD) was used to initially assess the structure of bulk samples of network β-CDMOF-1. Comparison of the PXRD patterns of β-CDMOF-**1** (red) showed similarities to the calculated pattern from SC-XRD (bottom; blue). When crystals were soaked twice with ethanol for 24 hours each, followed by two further 24 hour DCM cycles and isolation in-vacuo resulted in the overall shape resembling the calculated pattern. Admittedly, solvent loss greatly diminished the crystallinity of the material.

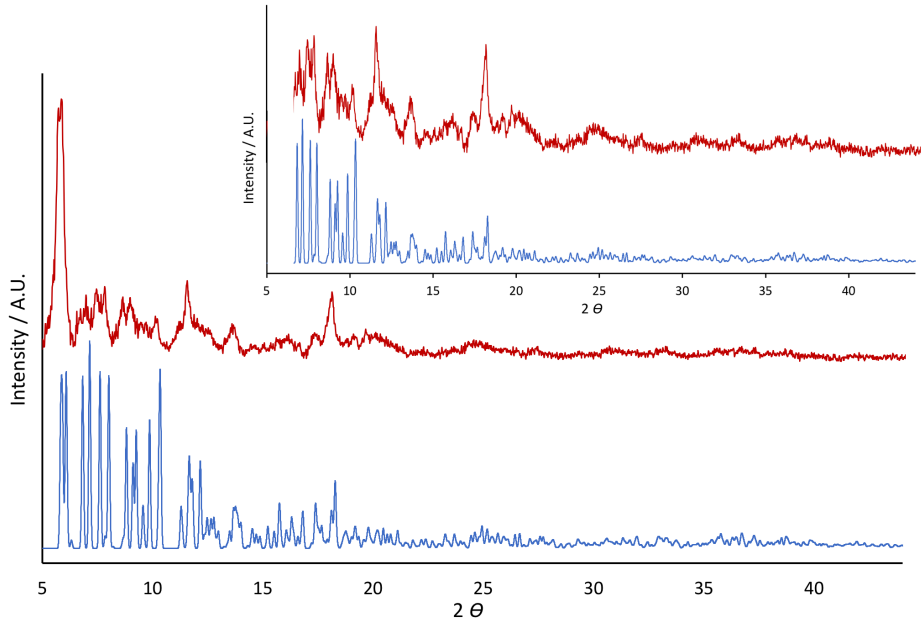

Fig. S1 PXRD comparison of β-CDMOF-1, Calculated theoretical pattern from SC-XRD (bottom; blue), β-CDMOF-**1** soaked in EtOH, then DCM and evacuated (top; red). Inset: expanded view of pattern above 7 degrees 2θ

S4. Thermogravimetric Analysis

Thermogravimetric analysis (TGA) was performed on all the MOFs (Figures S2 and S3) to determine their thermal stabilities. Measurements were carried out under an air atmosphere, resulting in decomposition of the Cyclodextrin occurring from 250°C.

Figure S2 shows the plotted data for the TGA analysis of β-CDMOF-1 following an ethanol soak, and dried under vacuum; here we recorded the loss in mass with respect to increase in

temperature. The initial sample mass was 27.4 mg. As the temperature increased from 30-100°C a loss of 10% was observed and was due to loss of residual solvent within the crystals as the boiling points of methanol/ethanol/water were up to 100°C. A 50% mass loss was observed in the region of 220-320°C this was due to the thermal degradation of β-Cyclodextrin.[S7]

Figure S3 shows the plotted data for the TGA analysis of β-CDMOF-1 following the ethanol/DCM soaking protocols and dried under vacuum. The initial sample mass was 21.3 mg. As the temperature increased from 30-100°C a loss of ~5% was observed and was due to loss of included water molecules (13 water molecules per unit cell; $9OH^-$ that react at elevated temperatures to form $9H_2O$ and 4 lattice H_2O molecules) within the crystals as the boiling points of 100°C. A 50% mass loss was observed in the region of 220-320°C this was due to the thermal degradation of β-Cyclodextrin.[S7] The mass loss (5%) is consistent with 9+4 hydroxyl/water content observed in the CHN analysis.

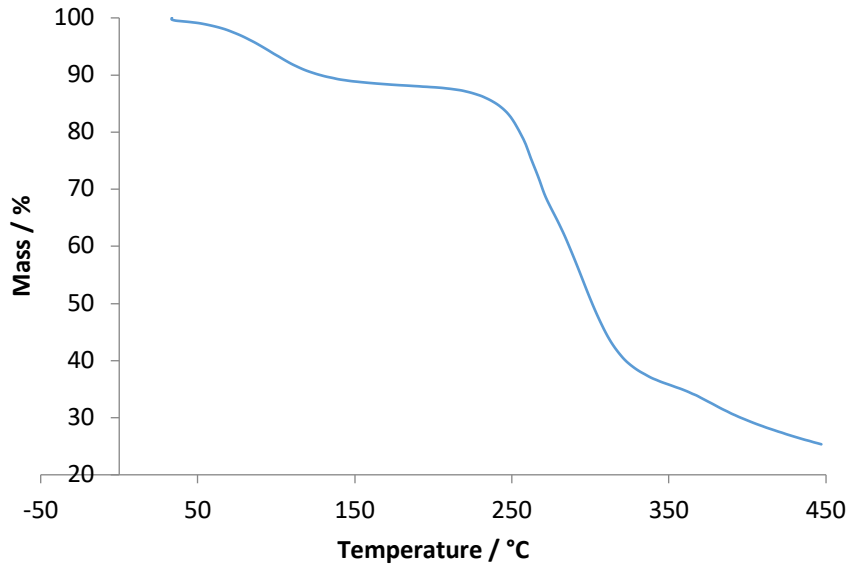

Fig. S2 Thermogravimetric analysis of β-CDMOF-1 following ethanol soaking protocol and desolvated *in vacuo*.

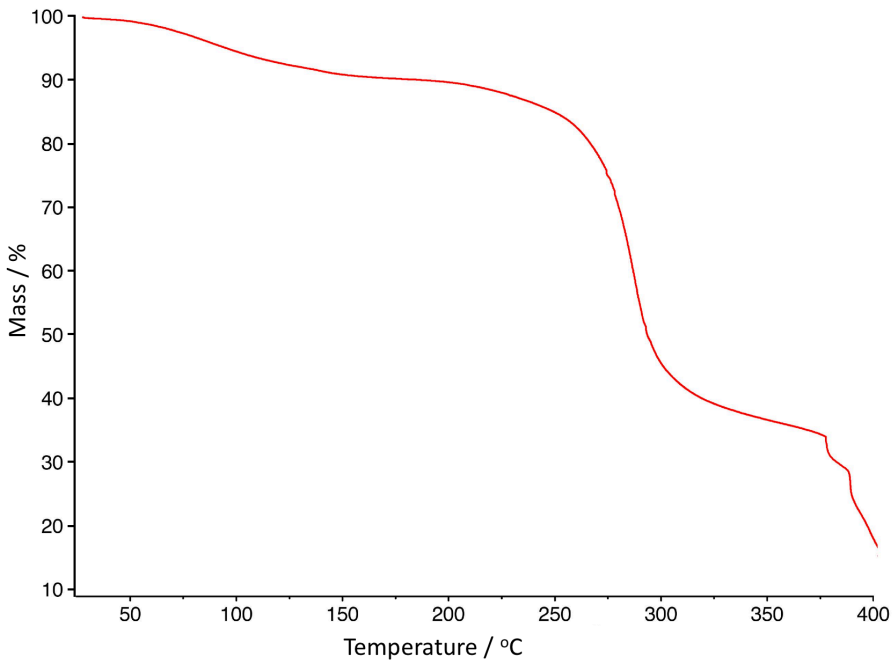

Fig. S3 Thermogravimetric analysis of β-CDMOF-1 following ethanol/DCM soaking protocol and desolvated *in vacuo*.

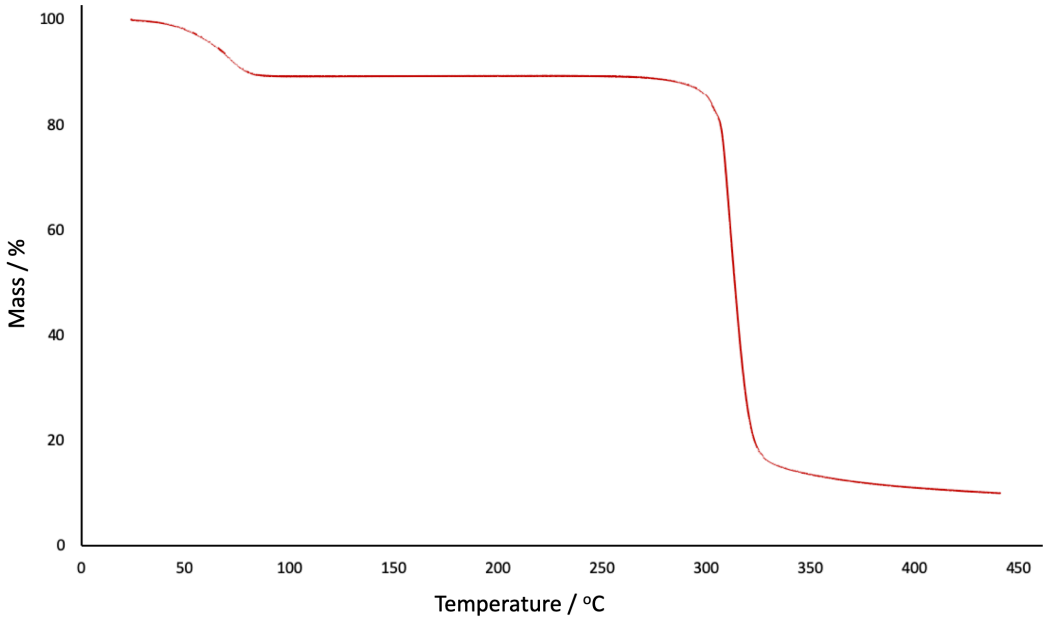

Fig. S4 Thermogravimetric analysis of commercial β-CD.

S5. Cholesterol Uptake By β-CD network

The crystal structure of β-CDMOF-1 showed continuous channels which closely resembled carbon nanotubes. β-CD is known to effectively bind nonpolar molecules and many works have been published using cholesterol with methyl-β-CD. A logical progression from this was to examine liquid to solid uptake of molecular cholesterol into the β-CDMOF-1 channels. Initially a stock solution of cholesterol (5 mM) was made in ethanol. 2 mL of this solution was added to β-CDMOF-1 crystals to see if any changes occurred. Crystals of β-CD were also soaked in ethanolic cholesterol and both imaged over 24hrs by optical microscopy .

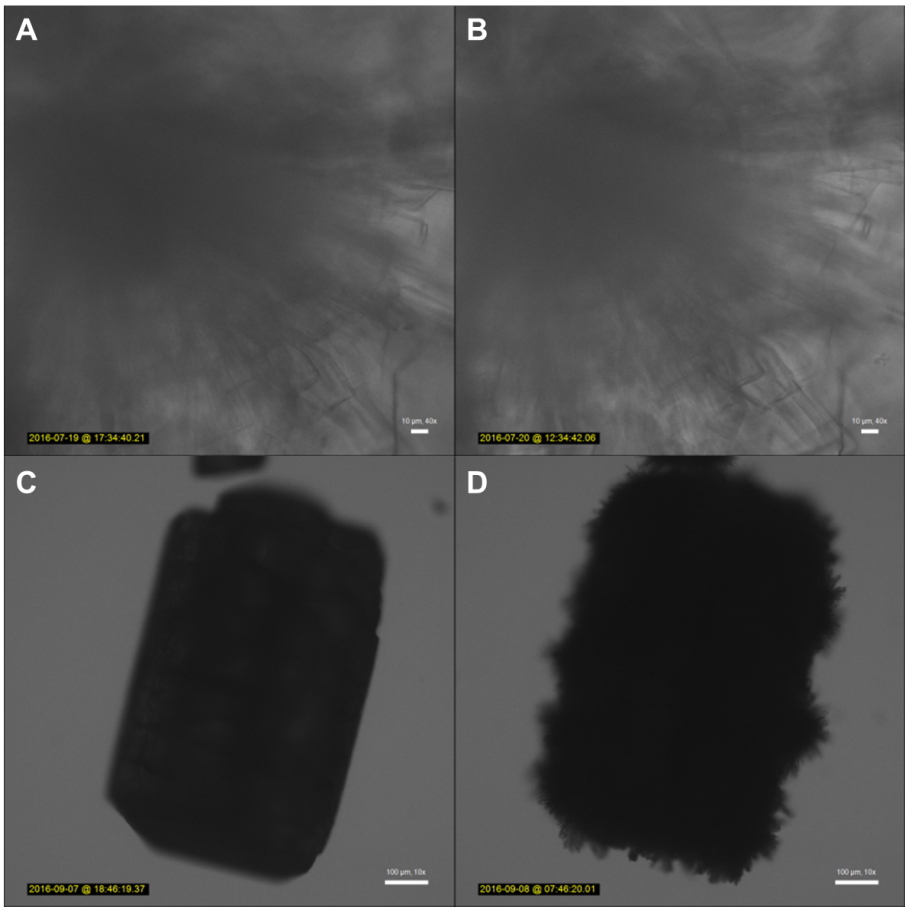

Fig. S5 Images of a β-CDMOF-1 crystal before (A) and after (B) soaking in cholesterol solution (scale bars for A and B = 10 um). Image of β-CD crystal before (C) and after (D) soaking in cholesterol solution (Scale bars for A and B = 100 um).

The results showed that after a period of 24 hours soaking, new crystalline material had nucleated on the entire surface of the β-CDMOF-1 crystals. Single crystal diffraction analysis of these hybrid crystals revealed a single crystal pattern indistinguishable from that of β-CD,

superimposed with a powder diffraction pattern of cholesterol originating in the crystallites that had grown on the surface. This indicates that cholesterol does not penetrate into β-CD crystals, rather interacting with the surface only. In this case, the apertures of the β-CD crystals are two β-CD units deep and then blocked by the offset alignment provided by the innate herringbone topology. On the other hand, β-CDMOF-1 remained unchanged before and after soaking. Diffraction data could not discern between disordered solvent or disordered guest cholesterol however, no evidence of surface cholesterol crystallisation was observed, but uptake by β-CDMOF-1 would require an alternative technique to confirm molecular absorption into the tubular solid.

S6. Sterol Uptake by β-CD Network - ^{1}H NMR Uptake Ratio Studies

^{1}H NMR experiments were undertaken to quantify the uptake of cholesterol and structurally similar sterols by the K^{+} β-CD MOF. MOF crystals were soaked in ethanolic cholesterol (2 mL, 5 mM) for 24 hours, before being removed from the solution, gently rinsed with ethanol and digested into NMR solvent (1:1 mix of methanol-d_4 and DMSO-d_6). The ratio of sterol molecules to β-cyclodextrin molecules could then be determined by using the integrations of distinct functional groups on the respective compounds. In the case of β-CD there are seven glycosidic protons per molecule at 4.8ppm (Figure S5, purple), and six isopropyl/ three aromatic/ nine methyl protons for cholesterol, β-estradiol and deoxycholic acid were scrutinised respectively (Figure S5, orange). The relative integrations of these peaks allowed for a ratio of sterol to cyclodextrin to be determined. These ratios were calculated to be 1 cholesterol molecule to 2 CD units; 1 β-estradiol molecule to 2 CD units and 1 deoxycholic acid to 3 CD units.

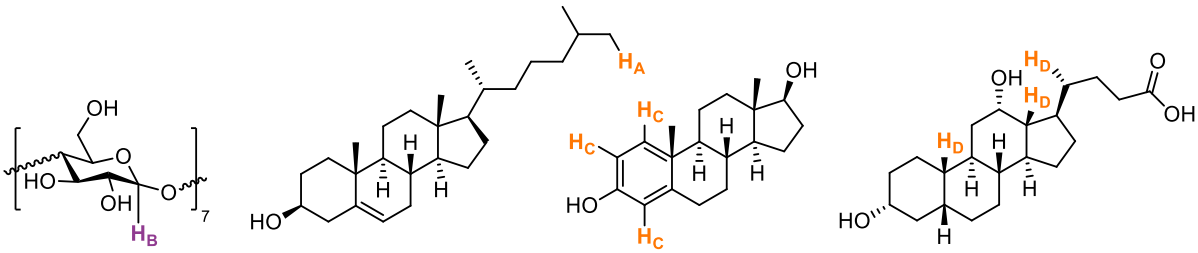

ß-Cyclodextrin Cholesterol ß Estradiol Deoxycholic Acid

Fig. S6 Molecular structures of β-CD and the three sterols that were used in this study, with relevant proton environments (H_A-H_D) highlighted in purple and orange.

Uptake of Cholesterol

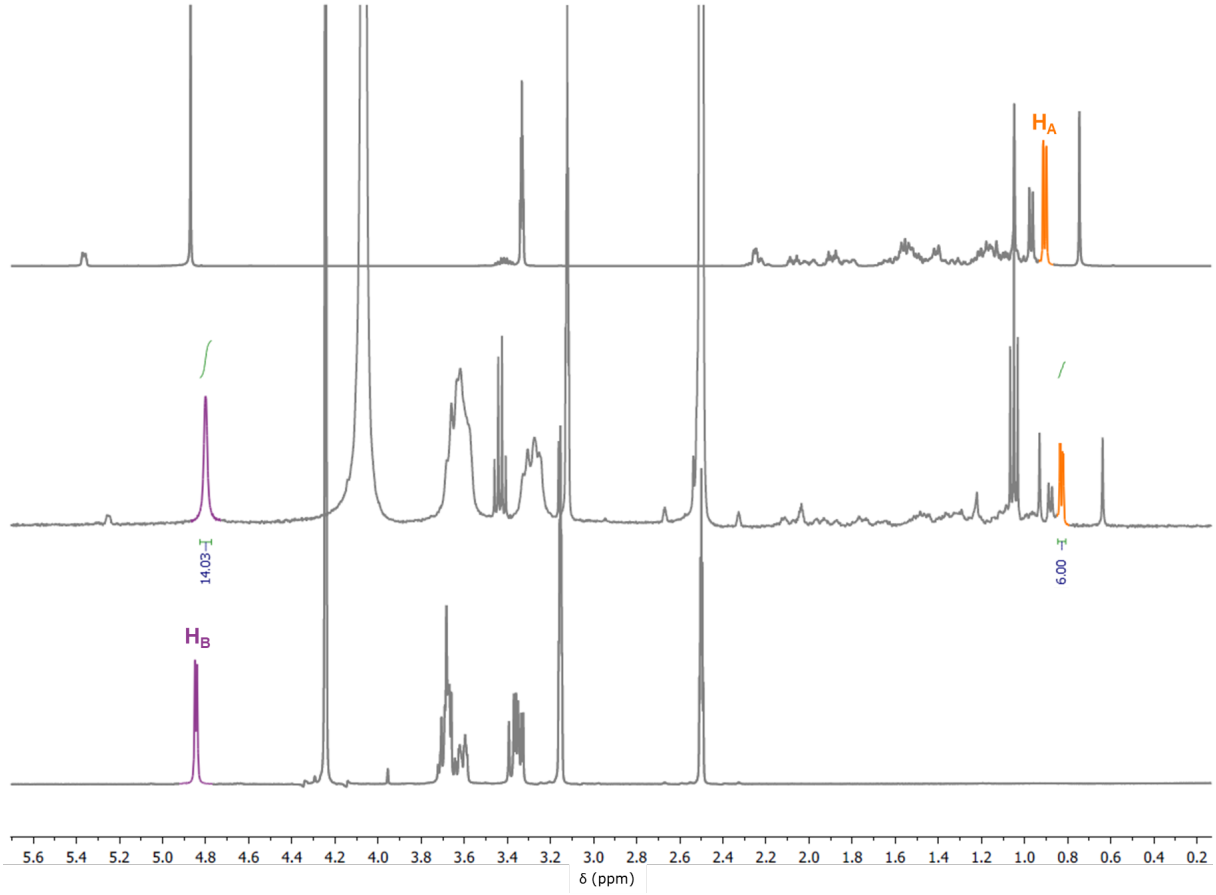

Fig. S7 NMR spectra of cholesterol (methanol-d_4, 400 MHz, top)**,** β-CDMOF-1 crystals after soaking in ethanolic cholesterol (digested in methanol-d_4/ DMSO-d_6, 400 MHz, middle) and β-CD (methanol-d_4/ DMSO-d_6, 400 MHz, bottom).

The six protons on the isopropyl group of cholesterol were used as a reference and corresponded to 14 glycosidic protons from β-CD. Given that one β-CD molecule has seven protons of this type, the ratio of cholesterol to β-CD unit in the formed inclusion complex is 1:2.

Uptake of β-Estradiol

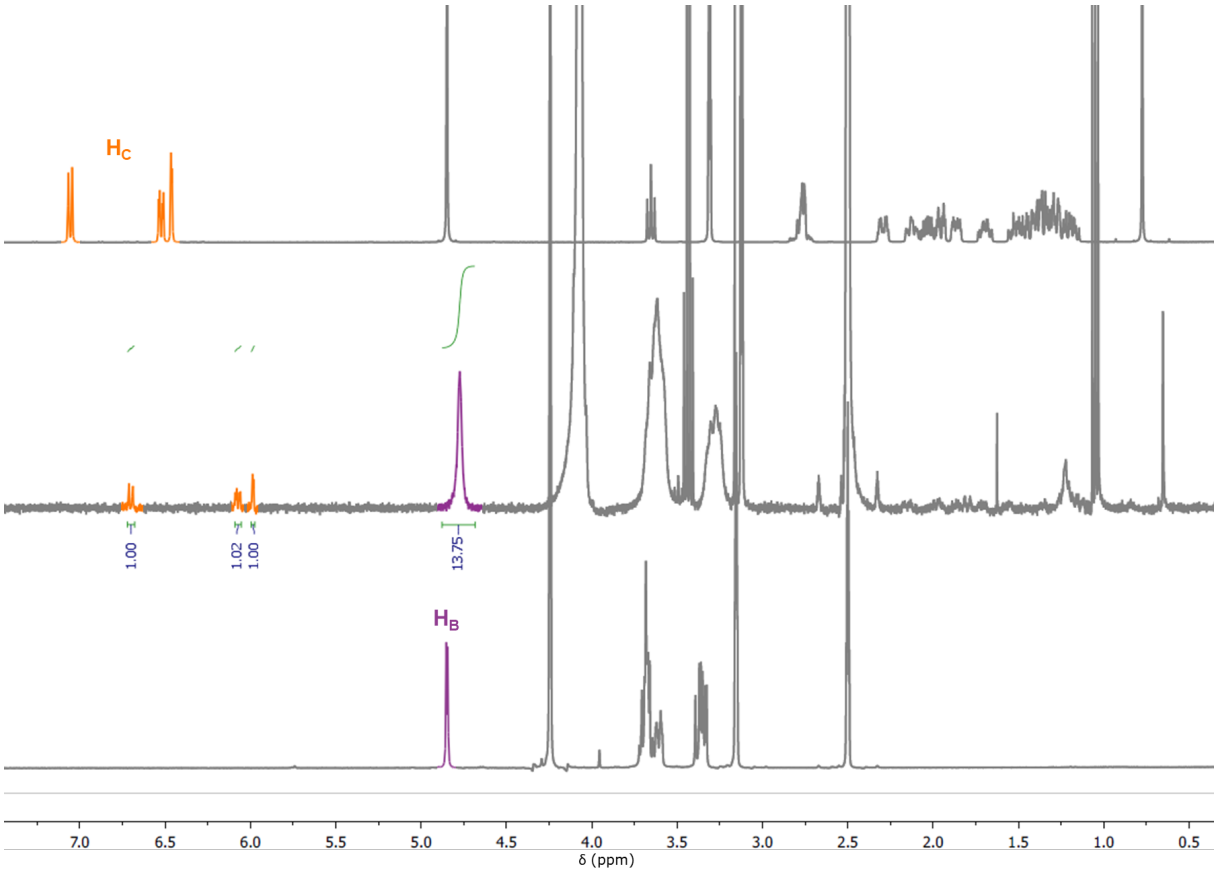

Fig. S8 NMR spectra of β-estradiol (methanol-d_4, 400 MHz, top), β-CDMOF-1 crystals after soaking in ethanolic β-estradiol (digested in methanol-d_4/ DMSO-d_6, 400 MHz, middle) and β-CD (methanol-d_4/ DMSO-d_6, 400 MHz, bottom).

β-Estradiol features a tri-substituted benzene that gave a unique set of distinguishing peaks in the ^{1}H NMR spectrum within the range of 6-7 ppm. With these aromatic protons as a reference, the ratio of β-estradiol to β-CD was 1:13.75 (~1:14). With seven glycosidic protons per β-CD molecule, the ratio of β-estradiol to β-CD in this inclusion complex is 1:2.

Uptake of Deoxycholic Acid

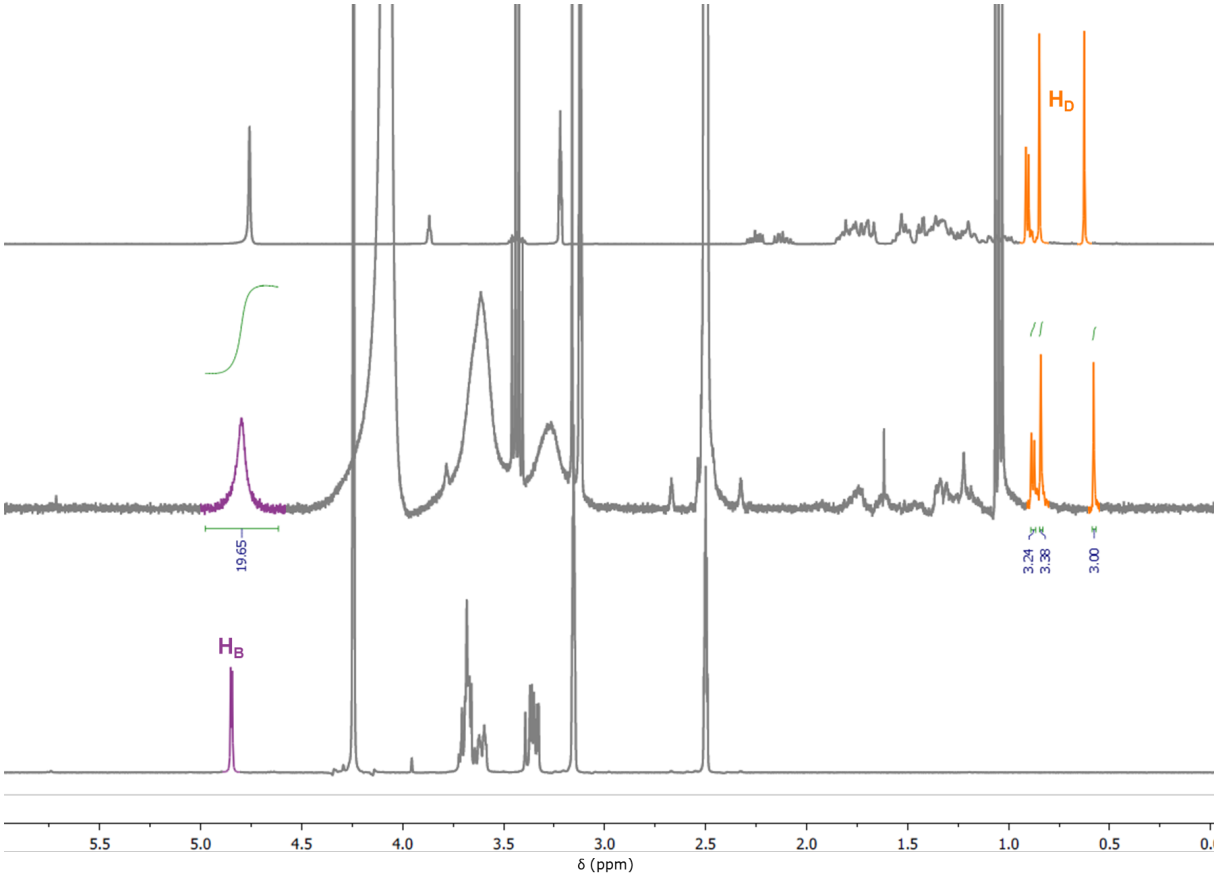

Fig. S9 NMR spectra of deoxycholic acid (methanol-d_4, 400 MHz, top), β-CDMOF-1 crystals after soaking in ethanolic deoxycholic acid (digested in methanol-d_4/ DMSO-d_6, 400 MHz, middle) and β-CD (methanol-d_4/ DMSO-d_6, 400 MHz, bottom).

Protons on three separate methyl groups on deoxycholic acid were used as a reference and corresponded to 19.65 glycosidic protons from β-CD (~3:21). With seven glycosidic protons per β-CD molecule, the ratio of deoxycholic acid to β-CD units in the formed inclusion complex is approximately 1:3.

The results obtained in these uptake studies show that the β-CDMOF-1 network is able to sequester cholesterol and structurally similar sterols from solution.

S7. Fluorescence Confocal Microscopy

Fluorescently-labelled MOFs were imaged on 35 mm glass bottom dishes (MatTek, Ashland, MA, USA) at room temperature. Images were collected on an LSM 880 Elyra (Zeiss, Jena, Germany) confocal microscope using a 20x Plan-Apochromat objective (Zeiss) in Z-series Airyscan super-resolution mode. TopFluor-Cholesterol (Avanti, Alabaster, AL, USA) was imaged using the 488nm line, a 488 nm main beam splitter and a 495-620 nm band-pass emission filter. Resorufin (Sigma Aldrich) was imaged using the 561 nm laser line, a 458/561 nm main beam splitter and a 570-620 nm band-pass emission filter. Post-imaging processing and export was performed in the Zen (Zeiss) software package, with manipulations limited to image cropping and even adjustments of image levels across the entire image.

S8. References

[S1]. G. M. Sheldrick, Acta Crystallogr., Sect. A: Found. Adv., 2015, 71, 3–8. 17

[S2]. G. M. Sheldrick, Acta Crystallogr., Sect. C: Struct. Chem., 2015, 71, 3–8. 18

[S3]. O. V. Dolomanov, L. J. Bourhis, R. J. Gildea, J. A. K. Howard and H. Puschmann, J. Appl. Crystallogr., 2009, 42, 339–341

[S4]. *CrysAlis Pro*, Rigaku Oxford Diffraction, Kent, U.K.

[S5]. *Apex2*, Bruker AXS Inc., Madison, Wisconsin, U.S.A.

[S6]. *SADABS*, Bruker AXS Inc., Madison, Wisconsin, USA.

[S7]. Trotta, F., Zanetti, M. and Camino, G. (2000), Polymer Degradation and Stability, Vol.69(3), 373-379

checkCIF/PLATON report

You have not supplied any structure factors. As a result the full set of tests cannot be run.

THIS REPORT IS FOR GUIDANCE ONLY. IF USED AS PART OF A REVIEW PROCEDURE FOR PUBLICATION, IT SHOULD NOT REPLACE THE EXPERTISE OF AN EXPERIENCED CRYSTALLOGRAPHIC REFEREE.

No syntax errors found. CIF dictionary Interpreting this report

Datablock: b-CDMOF-1

```
Bond precision:  C-C = 0.0173 A          Wavelength=0.88560

Cell:          a=15.2438(6)       b=15.2742(6)     c=29.7686(13)
               alpha=101.314(2)   beta=94.845(2)   gamma=95.071(2)
Temperature:   100 K
```

	Calculated	Reported
Volume	6733.1(5)	6733.1(5)
Space group	P 1	P 1
Hall group	P 1	P 1
Moiety formula	C168 H280 K9 O149, 2(C H4 O), 13(O)	2.25(K), C42 H70 O35, 5.5(O), 0.5(C H4 O)
Sum formula	C170 H288 K9 O164	C42.50 H72 K2.25 O41
Mr	5307.84	1326.97
Dx,g cm-3	1.309	1.309
Z	1	4
Mu (mm-1)	0.452	0.462
F000	2791.0	2791.0
F000’	2797.00	
h,k,lmax	19,19,37	19,19,37
Nref	55448[27724]	50757
Tmin,Tmax		0.413,0.747
Tmin’		

```
Correction method= # Reported T Limits: Tmin=0.413 Tmax=0.747
AbsCorr = MULTI-SCAN

Data completeness= 1.83/0.92      Theta(max)= 33.695

R(reflections)= 0.1136( 35439)    wR2(reflections)= 0.3268( 50757)

S = 1.034                  Npar= 3178
```

The following ALERTS were generated. Each ALERT has the format
test-name_ALERT_alert-type_alert-level.
Click on the hyperlinks for more details of the test.

Alert level A

PLAT602_ALERT_2_A VERY LARGE Solvent Accessible VOID(S) in Structure ! Info

Author Response: The large voids are key to the chemistry and are discussed extensively in the accompanying publication.

Alert level B

```
PLAT097_ALERT_2_B Large Reported Max.  (Positive) Residual Density       2.35 eA-3
PLAT220_ALERT_2_B Non-Solvent  Resd 1  O   Ueq(max)/Ueq(min) Range        7.3 Ratio
PLAT306_ALERT_2_B Isolated Oxygen Atom (H-atoms Missing ?) .......        O1S Check
PLAT306_ALERT_2_B Isolated Oxygen Atom (H-atoms Missing ?) .......        O3S Check
PLAT306_ALERT_2_B Isolated Oxygen Atom (H-atoms Missing ?) .......        O4S Check
PLAT306_ALERT_2_B Isolated Oxygen Atom (H-atoms Missing ?) .......        O8S Check
PLAT306_ALERT_2_B Isolated Oxygen Atom (H-atoms Missing ?) .......        O9S Check
PLAT306_ALERT_2_B Isolated Oxygen Atom (H-atoms Missing ?) .......       O11S Check
PLAT306_ALERT_2_B Isolated Oxygen Atom (H-atoms Missing ?) .......       O12S Check
PLAT306_ALERT_2_B Isolated Oxygen Atom (H-atoms Missing ?) .......       O15S Check
PLAT306_ALERT_2_B Isolated Oxygen Atom (H-atoms Missing ?) .......       O17S Check
PLAT306_ALERT_2_B Isolated Oxygen Atom (H-atoms Missing ?) .......       O18S Check
PLAT306_ALERT_2_B Isolated Oxygen Atom (H-atoms Missing ?) .......       O20S Check
PLAT306_ALERT_2_B Isolated Oxygen Atom (H-atoms Missing ?) .......       O21S Check
PLAT306_ALERT_2_B Isolated Oxygen Atom (H-atoms Missing ?) .......       O22S Check
PLAT340_ALERT_3_B Low Bond Precision on  C-C Bonds ...............    0.01726 Ang.
PLAT417_ALERT_2_B Short Inter D-H..H-D       H        ..H4CA     .       2.09 Ang.
                                                    x,1+y,z  =      1_565 Check
PLAT420_ALERT_2_B D-H Without Acceptor       O13A     --Ha       .     Please Check
PLAT420_ALERT_2_B D-H Without Acceptor       O5B      --H5B      .     Please Check
PLAT420_ALERT_2_B D-H Without Acceptor       O10B     --H10B     .     Please Check
PLAT420_ALERT_2_B D-H Without Acceptor       O9A      --Hl       .     Please Check
PLAT420_ALERT_2_B D-H Without Acceptor       O24A     --Hm       .     Please Check
PLAT420_ALERT_2_B D-H Without Acceptor       O18B     --H18B     .     Please Check
PLAT420_ALERT_2_B D-H Without Acceptor       O20B     --H20B     .     Please Check
PLAT420_ALERT_2_B D-H Without Acceptor       O24B     --H24B     .     Please Check
PLAT420_ALERT_2_B D-H Without Acceptor       O20      --H0AA     .     Please Check
PLAT420_ALERT_2_B D-H Without Acceptor       O25      --H7AA     .     Please Check
PLAT420_ALERT_2_B D-H Without Acceptor       O15      --H2BA     .     Please Check
PLAT420_ALERT_2_B D-H Without Acceptor       O33C     --H0CA     .     Please Check
PLAT420_ALERT_2_B D-H Without Acceptor       O5A      --H8CA     .     Please Check
PLAT420_ALERT_2_B D-H Without Acceptor       O35C     --H0EA     .     Please Check
PLAT420_ALERT_2_B D-H Without Acceptor       O25C     --H1EA     .     Please Check
PLAT420_ALERT_2_B D-H Without Acceptor       O30C     --H7JA     .     Please Check
PLAT420_ALERT_2_B D-H Without Acceptor       O5C      --H4OA     .     Please Check
PLAT430_ALERT_2_B Short Inter D...A Contact  O3S      ..O4S      .       2.80 Ang.
                                                      x,y,z  =      1_555 Check
PLAT430_ALERT_2_B Short Inter D...A Contact  O4S      ..O5S      .       2.81 Ang.
                                                    1+x,y,z  =      1_655 Check
PLAT430_ALERT_2_B Short Inter D...A Contact  O8S      ..O9S      .       2.72 Ang.
                                                    1+x,y,z  =      1_655 Check
PLAT430_ALERT_2_B Short Inter D...A Contact  O15S     ..O16S     .       2.78 Ang.
                                                      x,y,z  =      1_555 Check
PLAT430_ALERT_2_B Short Inter D...A Contact  O16S     ..O18S     .       2.81 Ang.
                                                      x,y,z  =      1_555 Check
PLAT430_ALERT_2_B Short Inter D...A Contact  O18S     ..O19S     .       2.84 Ang.
```

```
                                                x,-1+y,-1+z  =      1_544 Check
PLAT430_ALERT_2_B Short Inter D...A Contact  O20S     ..O21S     .       2.77 Ang.
                                                   x,-1+y,z  =      1_545 Check
PLAT780_ALERT_1_B Coordinates do not Form a Properly Connected Set     Please Do !
```

Alert level C

```
DIFMX02_ALERT_1_C  The maximum difference density is > 0.1*ZMAX*0.75
            The relevant atom site should be identified.
PLAT082_ALERT_2_C High R1 Value ..................................       0.11 Report
PLAT084_ALERT_3_C High wR2 Value (i.e. > 0.25) ...................       0.33 Report
PLAT094_ALERT_2_C Ratio of Maximum / Minimum Residual Density ....       2.57 Report
PLAT213_ALERT_2_C Atom O19             has ADP max/min Ratio .....        3.5 prolat
PLAT213_ALERT_2_C Atom O19B            has ADP max/min Ratio .....        3.4 prolat
PLAT213_ALERT_2_C Atom C25             has ADP max/min Ratio .....        3.1 oblate
PLAT220_ALERT_2_C Non-Solvent  Resd 1  C   Ueq(max)/Ueq(min) Range        3.3 Ratio
PLAT222_ALERT_3_C Non-Solv.  Resd 1  H   Uiso(max)/Uiso(min) Range        8.3 Ratio
PLAT241_ALERT_2_C High   'MainMol' Ueq as Compared to Neighbors of        O5C Check
PLAT241_ALERT_2_C High   'MainMol' Ueq as Compared to Neighbors of        O6S Check
PLAT241_ALERT_2_C High   'MainMol' Ueq as Compared to Neighbors of       O30C Check
PLAT242_ALERT_2_C Low    'MainMol' Ueq as Compared to Neighbors of         K2 Check
PLAT242_ALERT_2_C Low    'MainMol' Ueq as Compared to Neighbors of        C37 Check
PLAT260_ALERT_2_C Large Average Ueq of Residue Including      O20S      0.123 Check
PLAT417_ALERT_2_C Short Inter D-H..H-D       Hw       ..H6EA     .       2.10 Ang.
                                                     x,y,z  =      1_555 Check
PLAT430_ALERT_2_C Short Inter D...A Contact  O21S     ..O22S     .       2.85 Ang.
                                                 x,1+y,1+z  =      1_566 Check
```

Alert level G

```
ABSMU01_ALERT_1_G  Calculation of _exptl_absorpt_correction_mu
               not performed for this radiation type.
PLAT003_ALERT_2_G Number of Uiso or Uij Restrained non-H Atoms ...         12 Report
PLAT004_ALERT_5_G Polymeric Structure Found with Maximum Dimension          3 Info
PLAT007_ALERT_5_G Number of Unrefined Donor-H Atoms ..............         86 Report
PLAT012_ALERT_1_G N.O.K.   _shelx_res_checksum Found in CIF ......     Please Check
PLAT033_ALERT_4_G Flack x Value Deviates > 3.0 * sigma from Zero .      0.166 Note
PLAT042_ALERT_1_G Calc. and Reported MoietyFormula Strings  Differ     Please Check
PLAT045_ALERT_1_G Calculated and Reported Z Differ by a Factor ...       0.25 Check
PLAT072_ALERT_2_G SHELXL First  Parameter in WGHT  Unusually Large       0.19 Report
PLAT083_ALERT_2_G SHELXL Second Parameter in WGHT  Unusually Large      16.20 Why ?
PLAT092_ALERT_4_G Check: Wavelength Given is not Cu,Ga,Mo,Ag,In Ka    0.88560 Ang.
PLAT154_ALERT_1_G The s.u.'s on the Cell Angles are Equal ..(Note)      0.002 Degree
PLAT186_ALERT_4_G The CIF-Embedded .res File Contains ISOR Records          2 Report
PLAT650_ALERT_4_G SWAT Instruction Used to Model Solvent Disorder           ! Report
PLAT720_ALERT_4_G Number of Unusual/Non-Standard Labels ..........        226 Note
PLAT860_ALERT_3_G Number of Least-Squares Restraints .............        141 Note
PLAT984_ALERT_1_G The  K-f'=    0.2780 Deviates from the B&C-Value     0.2676 Check
PLAT984_ALERT_1_G The  O-f'=    0.0190 Deviates from the B&C-Value     0.0176 Check
PLAT985_ALERT_1_G The  K-f"=    0.4050 Deviates from the B&C-Value     0.3836 Check
```

```
   1 ALERT level A = Most likely a serious problem - resolve or explain
  42 ALERT level B = A potentially serious problem, consider carefully
  17 ALERT level C = Check. Ensure it is not caused by an omission or oversight
  19 ALERT level G = General information/check it is not something unexpected

  10 ALERT type 1 CIF construction/syntax error, inconsistent or missing data
```

```
  58 ALERT type 2 Indicator that the structure model may be wrong or deficient
   4 ALERT type 3 Indicator that the structure quality may be low
   5 ALERT type 4 Improvement, methodology, query or suggestion
   2 ALERT type 5 Informative message, check
```

Datablock: b-CDMOF2-Chol

Bond precision: C-C = 0.0118 A Wavelength=1.54184

Cell: a=15.73558(13) b=24.3380(2) c=19.02257(18)
alpha=90 beta=107.6098(9) gamma=90
Temperature: 279 K

	Calculated	Reported
Volume	6943.73(11)	6943.73(11)
Space group	P 21	P 1 21 1
Hall group	P 2yb	P 2yb
Moiety formula	C84 H140 K2.55 O74.50, 0.32(C27 H45 O), O0.50, O0.50, O0.50, 2(	2.55(K), 2(C42 H70 O35), 12.5(O), 0.32(C27 H45 O)
Sum formula	C92.64 H154.40 K2.55 O82.82	C92.64 H154.40 K2.56 O82.82
Mr	2693.23	2693.25
Dx,g cm-3	1.288	1.288
Z	2	2
Mu (mm-1)	1.659	1.660
F000	2842.7	2843.0
F000’	2855.89	
h,k,lmax	18,28,22	18,28,22
Nref	24538[12586]	24281
Tmin,Tmax	0.741,0.819	0.806,1.000
Tmin’	0.672	

Correction method= # Reported T Limits: Tmin=0.806 Tmax=1.000
AbsCorr = MULTI-SCAN

Data completeness= 1.93/0.99 Theta(max)= 66.596

R(reflections)= 0.1025(22819) wR2(reflections)= 0.3033(24281)

S = 1.421 Npar= 1661

The following ALERTS were generated. Each ALERT has the format
test-name_ALERT_alert-type_alert-level.
Click on the hyperlinks for more details of the test.

Alert level B

```
PLAT306_ALERT_2_B Isolated Oxygen Atom (H-atoms Missing ?) .......        O2S Check
PLAT306_ALERT_2_B Isolated Oxygen Atom (H-atoms Missing ?) .......        O7S Check
PLAT306_ALERT_2_B Isolated Oxygen Atom (H-atoms Missing ?) .......       O10S Check
PLAT306_ALERT_2_B Isolated Oxygen Atom (H-atoms Missing ?) .......       O11S Check
PLAT306_ALERT_2_B Isolated Oxygen Atom (H-atoms Missing ?) .......       O13S Check
PLAT340_ALERT_3_B Low Bond Precision on  C-C Bonds ...............    0.01176 Ang.
PLAT420_ALERT_2_B D-H Without Acceptor       O1A      --H1A      .     Please Check
PLAT420_ALERT_2_B D-H Without Acceptor       O3B      --Hm       .     Please Check
PLAT420_ALERT_2_B D-H Without Acceptor       O16B     --H9DA     .     Please Check
PLAT430_ALERT_2_B Short Inter D...A Contact  O1       ..O2       .       2.56 Ang.
                                                      x,y,z  =      1_555 Check
PLAT430_ALERT_2_B Short Inter D...A Contact  O1       ..O3       .       2.68 Ang.
                                                 -1+x,y,-1+z  =      1_454 Check
PLAT430_ALERT_2_B Short Inter D...A Contact  O0AA     ..O10S     .       2.75 Ang.
                                                1-x,1/2+y,-z  =      2_655 Check
PLAT430_ALERT_2_B Short Inter D...A Contact  O2S      ..O3S      .       2.79 Ang.
                                               2-x,1/2+y,1-z  =      2_756 Check
PLAT430_ALERT_2_B Short Inter D...A Contact  O2AA     ..O4S      .       2.73 Ang.
                                                      x,y,z  =      1_555 Check
PLAT430_ALERT_2_B Short Inter D...A Contact  O4S      ..O10S     .       2.62 Ang.
                                                1-x,1/2+y,-z  =      2_655 Check
PLAT430_ALERT_2_B Short Inter D...A Contact  O4S      ..O5S      .       2.70 Ang.
                                                1-x,1/2+y,-z  =      2_655 Check
PLAT430_ALERT_2_B Short Inter D...A Contact  O5S      ..O11S     .       2.77 Ang.
                                                      x,y,z  =      1_555 Check
PLAT430_ALERT_2_B Short Inter D...A Contact  O6S      ..O11S     .       2.81 Ang.
                                                      x,y,z  =      1_555 Check
```

Alert level C

```
DIFMN02_ALERT_2_C  The minimum difference density is < -0.1*ZMAX*0.75
            _refine_diff_density_min given =     -1.439
            Test value =     -1.425
DIFMN03_ALERT_1_C  The minimum difference density is < -0.1*ZMAX*0.75
            The relevant atom site should be identified.
PLAT018_ALERT_1_C _diffrn_measured_fraction_theta_max .NE. *_full           ! Check
PLAT041_ALERT_1_C Calc. and Reported SumFormula    Strings  Differ     Please Check
PLAT077_ALERT_4_C Unitcell Contains Non-integer Number of Atoms ..     Please Check
PLAT084_ALERT_3_C High wR2 Value (i.e. > 0.25) ...................       0.30 Report
PLAT090_ALERT_3_C Poor Data / Parameter Ratio (Zmax > 18) ........       7.58 Note
PLAT098_ALERT_2_C Large Reported Min.  (Negative) Residual Density      -1.44 eA-3
PLAT213_ALERT_2_C Atom O6A             has ADP max/min Ratio .....        3.1 prolat
PLAT213_ALERT_2_C Atom C1B             has ADP max/min Ratio .....        3.2 prolat
PLAT213_ALERT_2_C Atom C7A             has ADP max/min Ratio .....        3.4 prolat
PLAT220_ALERT_2_C Non-Solvent  Resd 1  C   Ueq(max)/Ueq(min) Range        3.1 Ratio
PLAT220_ALERT_2_C Non-Solvent  Resd 1  O   Ueq(max)/Ueq(min) Range        4.5 Ratio
PLAT222_ALERT_3_C Non-Solv.  Resd 1  H   Uiso(max)/Uiso(min) Range        5.4 Ratio
PLAT241_ALERT_2_C High   'MainMol' Ueq as Compared to Neighbors of         K1 Check
PLAT242_ALERT_2_C Low    'MainMol' Ueq as Compared to Neighbors of       O11B Check
PLAT242_ALERT_2_C Low    'MainMol' Ueq as Compared to Neighbors of        C1A Check
PLAT309_ALERT_2_C Single Bonded Oxygen (C-O > 1.3 Ang) ...........        O1C Check
PLAT410_ALERT_2_C Short Intra H...H Contact  Hx       ..H5DA     .       1.97 Ang.
                                                      x,y,z  =      1_555 Check
PLAT414_ALERT_2_C Short Intra D-H..H-X       H3CA     ..H4EA             1.98 Ang.
                                                      x,y,z  =      1_555 Check
PLAT415_ALERT_2_C Short Inter D-H..H-X       Hm       ..H6AA     .       2.02 Ang.
                                             1-x,-1/2+y,1-z  =      2_646 Check
PLAT415_ALERT_2_C Short Inter D-H..H-X       H26A     ..Hz       .       2.12 Ang.
                                             1-x,-1/2+y,1-z  =      2_646 Check
PLAT416_ALERT_2_C Short Intra D-H..H-D       Hb       ..H7A      .       1.97 Ang.
                                                      x,y,z  =      1_555 Check
```

```
PLAT430_ALERT_2_C Short Inter D...A Contact  O1       ..O13S     .       2.86 Ang.
                                            1-x,-1/2+y,-z  =      2_645 Check
PLAT430_ALERT_2_C Short Inter D...A Contact  O0AA     ..O8S      .       2.88 Ang.
                                                  x,y,-1+z  =      1_554 Check
PLAT601_ALERT_2_C Structure Contains Solvent Accessible VOIDS of .         74 Ang**3
```

Alert level G

```
PLAT002_ALERT_2_G Number of Distance or Angle Restraints on AtSite         29 Note
PLAT004_ALERT_5_G Polymeric Structure Found with Maximum Dimension          3 Info
PLAT005_ALERT_5_G No Embedded Refinement Details Found  in the CIF     Please Do !
PLAT007_ALERT_5_G Number of Unrefined Donor-H Atoms .............         43 Report
PLAT033_ALERT_4_G Flack x Value Deviates > 3.0 * sigma from Zero .      0.140 Note
PLAT042_ALERT_1_G Calc. and Reported MoietyFormula Strings  Differ     Please Check
PLAT068_ALERT_1_G Reported F000 Differs from Calcd (or Missing)...     Please Check
PLAT072_ALERT_2_G SHELXL First  Parameter in WGHT  Unusually Large       0.20 Report
PLAT142_ALERT_4_G s.u. on b - Axis Small or Missing .............    0.00020 Ang.
PLAT143_ALERT_4_G s.u. on c - Axis Small or Missing .............    0.00018 Ang.
PLAT300_ALERT_4_G Atom Site Occupancy of K3         Constrained at      0.554 Check
PLAT300_ALERT_4_G Atom Site Occupancy of O0AA       Constrained at        0.5 Check
PLAT300_ALERT_4_G Atom Site Occupancy of O3         Constrained at        0.5 Check
PLAT300_ALERT_4_G Atom Site Occupancy of O4S        Constrained at        0.5 Check
PLAT300_ALERT_4_G Atom Site Occupancy of O1C        Constrained at       0.32 Check
PLAT300_ALERT_4_G Atom Site Occupancy of C1C        Constrained at       0.32 Check
PLAT300_ALERT_4_G Atom Site Occupancy of C2C        Constrained at       0.32 Check
PLAT300_ALERT_4_G Atom Site Occupancy of C3C        Constrained at       0.32 Check
PLAT300_ALERT_4_G Atom Site Occupancy of C4C        Constrained at       0.32 Check
PLAT300_ALERT_4_G Atom Site Occupancy of C5C        Constrained at       0.32 Check
PLAT300_ALERT_4_G Atom Site Occupancy of C6C        Constrained at       0.32 Check
PLAT300_ALERT_4_G Atom Site Occupancy of C7C        Constrained at       0.32 Check
PLAT300_ALERT_4_G Atom Site Occupancy of C8C        Constrained at       0.32 Check
PLAT300_ALERT_4_G Atom Site Occupancy of C9C        Constrained at       0.32 Check
PLAT300_ALERT_4_G Atom Site Occupancy of C10C       Constrained at       0.32 Check
PLAT300_ALERT_4_G Atom Site Occupancy of C11C       Constrained at       0.32 Check
PLAT300_ALERT_4_G Atom Site Occupancy of C12C       Constrained at       0.32 Check
PLAT300_ALERT_4_G Atom Site Occupancy of C13C       Constrained at       0.32 Check
PLAT300_ALERT_4_G Atom Site Occupancy of C14C       Constrained at       0.32 Check
PLAT300_ALERT_4_G Atom Site Occupancy of C15C       Constrained at       0.32 Check
PLAT300_ALERT_4_G Atom Site Occupancy of C16C       Constrained at       0.32 Check
PLAT300_ALERT_4_G Atom Site Occupancy of C17C       Constrained at       0.32 Check
PLAT300_ALERT_4_G Atom Site Occupancy of C18C       Constrained at       0.32 Check
PLAT300_ALERT_4_G Atom Site Occupancy of C19C       Constrained at       0.32 Check
PLAT300_ALERT_4_G Atom Site Occupancy of C20C       Constrained at       0.32 Check
PLAT300_ALERT_4_G Atom Site Occupancy of C21C       Constrained at       0.32 Check
PLAT300_ALERT_4_G Atom Site Occupancy of C22C       Constrained at       0.32 Check
PLAT300_ALERT_4_G Atom Site Occupancy of C23C       Constrained at       0.32 Check
PLAT300_ALERT_4_G Atom Site Occupancy of C24C       Constrained at       0.32 Check
PLAT300_ALERT_4_G Atom Site Occupancy of C25C       Constrained at       0.32 Check
PLAT300_ALERT_4_G Atom Site Occupancy of C26C       Constrained at       0.32 Check
PLAT300_ALERT_4_G Atom Site Occupancy of C27C       Constrained at       0.32 Check
PLAT300_ALERT_4_G Atom Site Occupancy of H9EA       Constrained at       0.32 Check
PLAT300_ALERT_4_G Atom Site Occupancy of H0FA       Constrained at       0.32 Check
PLAT300_ALERT_4_G Atom Site Occupancy of H1FA       Constrained at       0.32 Check
PLAT300_ALERT_4_G Atom Site Occupancy of H2FA       Constrained at       0.32 Check
PLAT300_ALERT_4_G Atom Site Occupancy of H3FA       Constrained at       0.32 Check
PLAT300_ALERT_4_G Atom Site Occupancy of H4FA       Constrained at       0.32 Check
PLAT300_ALERT_4_G Atom Site Occupancy of H5FA       Constrained at       0.32 Check
PLAT300_ALERT_4_G Atom Site Occupancy of H6FA       Constrained at       0.32 Check
PLAT300_ALERT_4_G Atom Site Occupancy of H7FA       Constrained at       0.32 Check
PLAT300_ALERT_4_G Atom Site Occupancy of H8FA       Constrained at       0.32 Check
PLAT300_ALERT_4_G Atom Site Occupancy of H9FA       Constrained at       0.32 Check
```

```
PLAT300_ALERT_4_G Atom Site Occupancy of H0GA       Constrained at       0.32 Check
PLAT300_ALERT_4_G Atom Site Occupancy of H1GA       Constrained at       0.32 Check
PLAT300_ALERT_4_G Atom Site Occupancy of H2GA       Constrained at       0.32 Check
PLAT300_ALERT_4_G Atom Site Occupancy of H3GA       Constrained at       0.32 Check
PLAT300_ALERT_4_G Atom Site Occupancy of H4GA       Constrained at       0.32 Check
PLAT300_ALERT_4_G Atom Site Occupancy of H5GA       Constrained at       0.32 Check
PLAT300_ALERT_4_G Atom Site Occupancy of H6GA       Constrained at       0.32 Check
PLAT300_ALERT_4_G Atom Site Occupancy of H7GA       Constrained at       0.32 Check
PLAT300_ALERT_4_G Atom Site Occupancy of H8GA       Constrained at       0.32 Check
PLAT300_ALERT_4_G Atom Site Occupancy of H9GA       Constrained at       0.32 Check
PLAT300_ALERT_4_G Atom Site Occupancy of H0HA       Constrained at       0.32 Check
PLAT300_ALERT_4_G Atom Site Occupancy of H1HA       Constrained at       0.32 Check
PLAT300_ALERT_4_G Atom Site Occupancy of H2HA       Constrained at       0.32 Check
PLAT300_ALERT_4_G Atom Site Occupancy of H3HA       Constrained at       0.32 Check
PLAT300_ALERT_4_G Atom Site Occupancy of H4HA       Constrained at       0.32 Check
PLAT300_ALERT_4_G Atom Site Occupancy of H5HA       Constrained at       0.32 Check
PLAT300_ALERT_4_G Atom Site Occupancy of H6HA       Constrained at       0.32 Check
PLAT300_ALERT_4_G Atom Site Occupancy of H7HA       Constrained at       0.32 Check
PLAT300_ALERT_4_G Atom Site Occupancy of H8HA       Constrained at       0.32 Check
PLAT300_ALERT_4_G Atom Site Occupancy of H9HA       Constrained at       0.32 Check
PLAT300_ALERT_4_G Atom Site Occupancy of H0IA       Constrained at       0.32 Check
PLAT300_ALERT_4_G Atom Site Occupancy of H1IA       Constrained at       0.32 Check
PLAT300_ALERT_4_G Atom Site Occupancy of H2IA       Constrained at       0.32 Check
PLAT300_ALERT_4_G Atom Site Occupancy of H3IA       Constrained at       0.32 Check
PLAT300_ALERT_4_G Atom Site Occupancy of H4IA       Constrained at       0.32 Check
PLAT300_ALERT_4_G Atom Site Occupancy of H5IA       Constrained at       0.32 Check
PLAT300_ALERT_4_G Atom Site Occupancy of H6IA       Constrained at       0.32 Check
PLAT300_ALERT_4_G Atom Site Occupancy of H7IA       Constrained at       0.32 Check
PLAT300_ALERT_4_G Atom Site Occupancy of H8IA       Constrained at       0.32 Check
PLAT300_ALERT_4_G Atom Site Occupancy of H9IA       Constrained at       0.32 Check
PLAT300_ALERT_4_G Atom Site Occupancy of H0JA       Constrained at       0.32 Check
PLAT300_ALERT_4_G Atom Site Occupancy of H1JA       Constrained at       0.32 Check
PLAT300_ALERT_4_G Atom Site Occupancy of H2JA       Constrained at       0.32 Check
PLAT300_ALERT_4_G Atom Site Occupancy of H3JA       Constrained at       0.32 Check
PLAT300_ALERT_4_G Atom Site Occupancy of O1         Constrained at        0.5 Check
PLAT300_ALERT_4_G Atom Site Occupancy of O1S        Constrained at        0.5 Check
PLAT300_ALERT_4_G Atom Site Occupancy of O2         Constrained at        0.5 Check
PLAT300_ALERT_4_G Atom Site Occupancy of O2AA       Constrained at        0.5 Check
PLAT300_ALERT_4_G Atom Site Occupancy of O5S        Constrained at        0.5 Check
PLAT300_ALERT_4_G Atom Site Occupancy of O8S        Constrained at        0.5 Check
PLAT301_ALERT_3_G Main Residue  Disorder ..............(Resd  1  )         2% Note
PLAT302_ALERT_4_G Anion/Solvent/Minor-Residue Disorder (Resd  2  )       100% Note
PLAT302_ALERT_4_G Anion/Solvent/Minor-Residue Disorder (Resd  3  )       100% Note
PLAT302_ALERT_4_G Anion/Solvent/Minor-Residue Disorder (Resd  4  )       100% Note
PLAT302_ALERT_4_G Anion/Solvent/Minor-Residue Disorder (Resd  5  )       100% Note
PLAT302_ALERT_4_G Anion/Solvent/Minor-Residue Disorder (Resd  7  )       100% Note
PLAT302_ALERT_4_G Anion/Solvent/Minor-Residue Disorder (Resd  8  )       100% Note
PLAT302_ALERT_4_G Anion/Solvent/Minor-Residue Disorder (Resd 10  )       100% Note
PLAT303_ALERT_2_G Full Occupancy Atom H11A      with # Connections       1.55 Check
PLAT303_ALERT_2_G Full Occupancy Atom Hq        with # Connections       2.00 Check
PLAT311_ALERT_2_G Isolated Disordered Oxygen Atom (No H’s ?) .....         O1 Check
PLAT311_ALERT_2_G Isolated Disordered Oxygen Atom (No H’s ?) .....        O1S Check
PLAT311_ALERT_2_G Isolated Disordered Oxygen Atom (No H’s ?) .....         O2 Check
PLAT311_ALERT_2_G Isolated Disordered Oxygen Atom (No H’s ?) .....       O2AA Check
PLAT311_ALERT_2_G Isolated Disordered Oxygen Atom (No H’s ?) .....        O5S Check
PLAT311_ALERT_2_G Isolated Disordered Oxygen Atom (No H’s ?) .....        O8S Check
PLAT413_ALERT_2_G Short Inter XH3 .. XHn     H5CA     ..H0IA     .       1.91 Ang.
                                                     x,y,z  =      1_555 Check
PLAT414_ALERT_2_G Short Intra D-H..H-X       H1A      ..Hs               1.92 Ang.
                                                   -1+x,y,z  =      1_455 Check
PLAT720_ALERT_4_G Number of Unusual/Non-Standard Labels ..........        128 Note
PLAT721_ALERT_1_G Bond    Calc     0.85000, Rep     0.84000 Dev...       0.01 Ang.
```

```
              O1AA     -H1AE            1.555   1.555 ........     #  388 Check
PLAT789_ALERT_4_G Atoms with Negative _atom_site_disorder_group  #         30 Check
PLAT860_ALERT_3_G Number of Least-Squares Restraints .............        189 Note
PLAT870_ALERT_4_G ALERTS Related to Twinning Effects Suppressed ..          ! Info
PLAT883_ALERT_1_G No Info/Value for _atom_sites_solution_primary .     Please Do !
```

```
   0 ALERT level A = Most likely a serious problem - resolve or explain
  18 ALERT level B = A potentially serious problem, consider carefully
  26 ALERT level C = Check. Ensure it is not caused by an omission or oversight
 117 ALERT level G = General information/check it is not something unexpected

   7 ALERT type 1 CIF construction/syntax error, inconsistent or missing data
  48 ALERT type 2 Indicator that the structure model may be wrong or deficient
   6 ALERT type 3 Indicator that the structure quality may be low
  97 ALERT type 4 Improvement, methodology, query or suggestion
   3 ALERT type 5 Informative message, check
```

It is advisable to attempt to resolve as many as possible of the alerts in all categories. Often the minor alerts point to easily fixed oversights, errors and omissions in your CIF or refinement strategy, so attention to these fine details can be worthwhile. In order to resolve some of the more serious problems it may be necessary to carry out additional measurements or structure refinements. However, the purpose of your study may justify the reported deviations and the more serious of these should normally be commented upon in the discussion or experimental section of a paper or in the "special_details" fields of the CIF. checkCIF was carefully designed to identify outliers and unusual parameters, but every test has its limitations and alerts that are not important in a particular case may appear. Conversely, the absence of alerts does not guarantee there are no aspects of the results needing attention. It is up to the individual to critically assess their own results and, if necessary, seek expert advice.

Publication of your CIF in IUCr journals

A basic structural check has been run on your CIF. These basic checks will be run on all CIFs submitted for publication in IUCr journals (*Acta Crystallographica*, *Journal of Applied Crystallography*, *Journal of Synchrotron Radiation*); however, if you intend to submit to *Acta Crystallographica Section C* or *E* or *IUCrData*, you should make sure that full publication checks are run on the final version of your CIF prior to submission.

Publication of your CIF in other journals

Please refer to the *Notes for Authors* of the relevant journal for any special instructions relating to CIF submission.

PLATON version of 07/08/2019; check.def file version of 30/07/2019

Datablock b-CDMOF-1 - ellipsoid plot

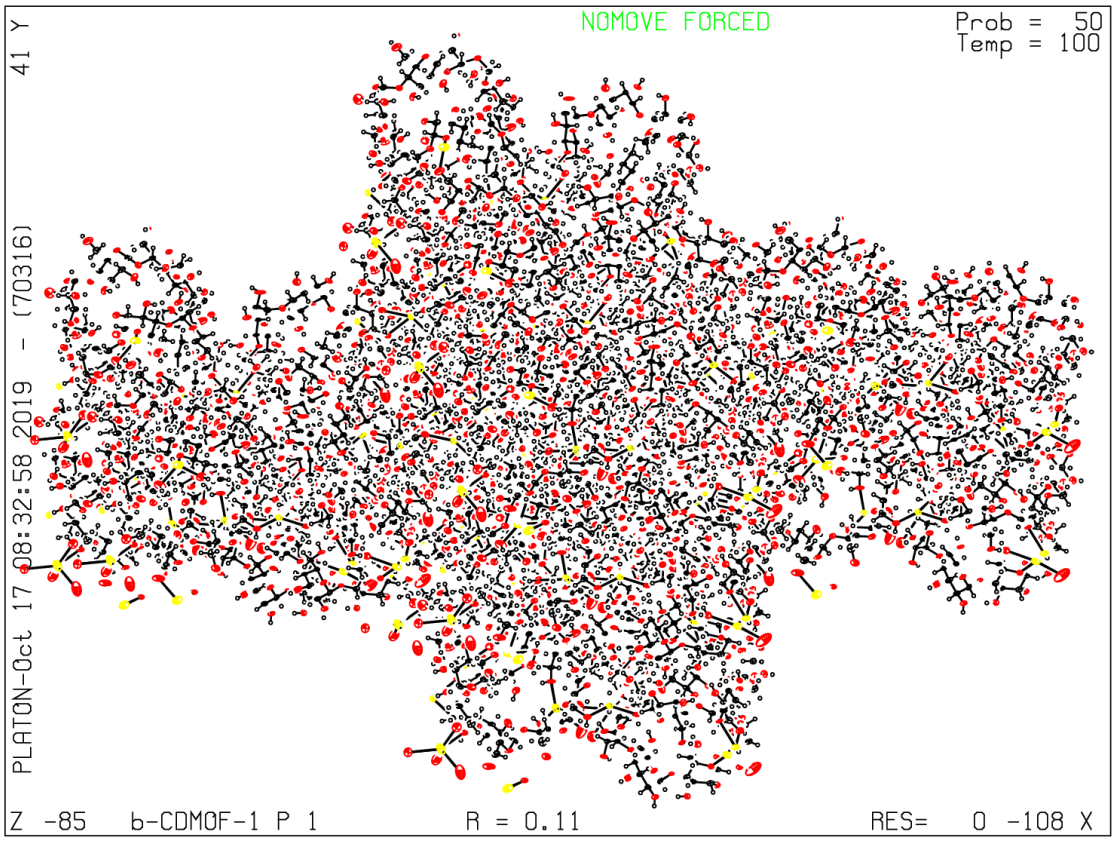

Datablock b-CDMOF2-Chol - ellipsoid plot

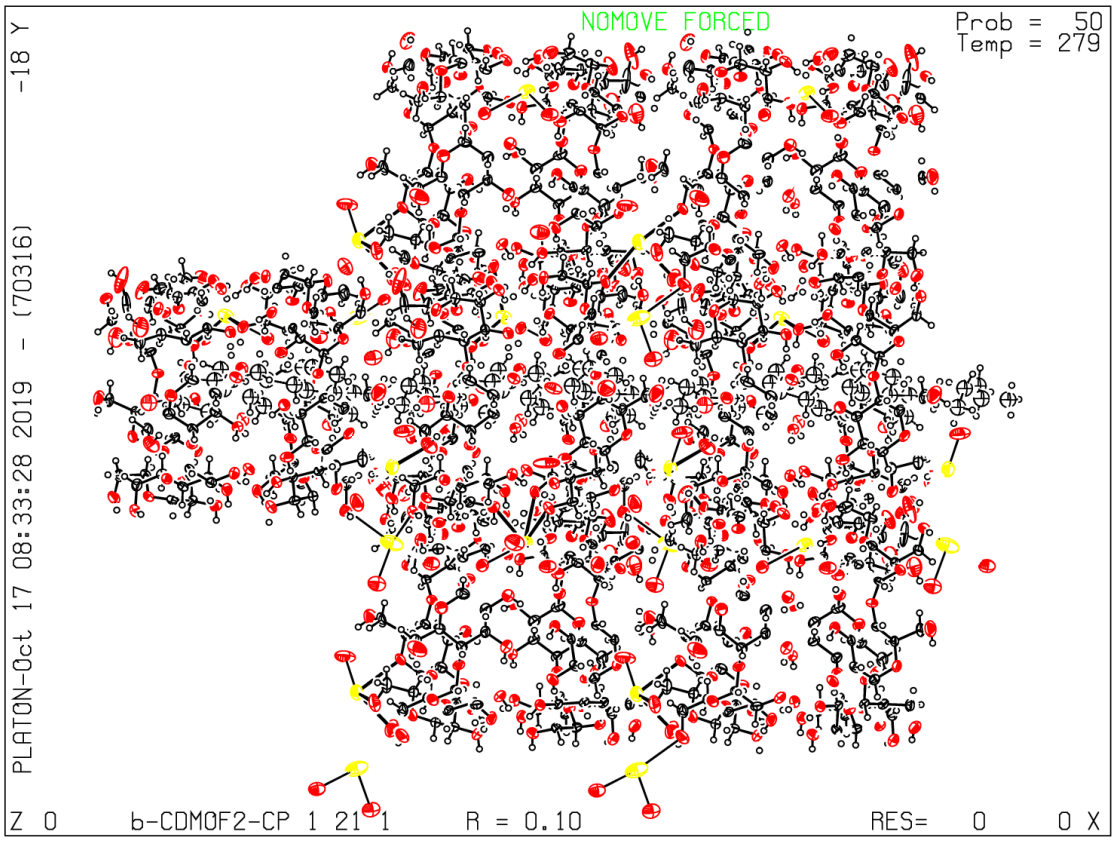

Other files

b-CDMOF_1-2chol_global.cif (2.11 MiB) view on ChemRxiv • download file